UDK 66:54(05) CODEN HMIDA 8 ISSN 0367–598X

2

Hemijska industrija

Vol. 80

Časopis Saveza hemijskih inženjera Srbije

Chemical Industry

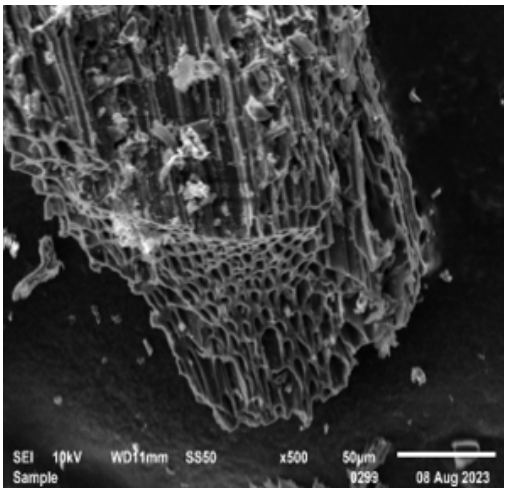

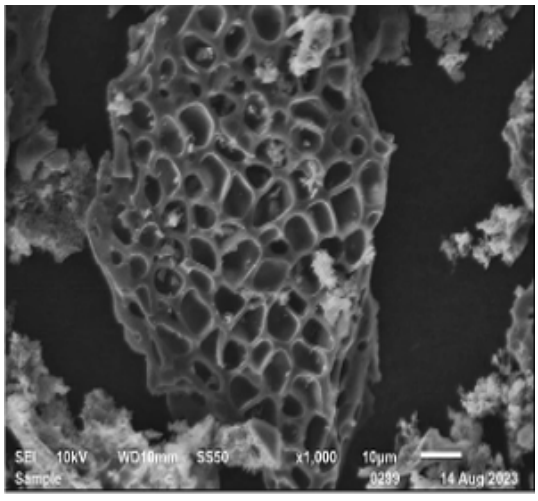

BEOGRAD, APRIL-JUNI 2026. HMIDA 8, 80(2) 71-115 (2026)

Aktivnosti Saveza hemijskih inženjera Srbije pomažu:

**MINISTARSTVO NAUKE,
TEHNOLOŠKOG RAZVOJA
I INOVACIJA
REPUBLIKE SRBIJE**

Tehnološko-metalurški fakultet
Univerziteta u Beogradu

Prirodno-matematički fakultet
Univerziteta u Novom Sadu

Tehnološki fakultet
Univerziteta u Novom Sadu

Fakultet tehničkih nauka
Univerziteta u Novom Sadu

Tehnološki fakultet
Univerziteta u Nišu, Leskovac

Institut IMS, Beograd

DCP HEMIGAL
Leskovac

Barič

Elixir Prahovo

VICTORIAOIL
Šid

Chemical Industry
Химическая промышленность

Hemijska industrija

Časopis Saveza hemijskih inženjera Srbije
Journal of the Association of Chemical Engineers of Serbia
Журнал Союза химических инженеров Сербии

VOL. 80 **Beograd, april - juni 2026.** **Broj 2**

Izdavač
Savez hemijskih inženjera Srbije
Beograd, Kneza Miloša 9/I

Glavni urednik
Bojana Obradović

Zamenica glavnog i odgovornog urednika
Emila Živković

Pomoćnik glavnog i odgovornog urednika
Ivana Drvenica

Urednici
Jelena Bajat, Dejan Bezbradica, Ivana Banković-Ilić, Dušan Mijin, Marija Nikolić, Đorđe Veljović, Tatjana Volkov-Husović

Članovi uredništva
Nikolaj Ostrovski, Milorad Cakić, Željko Čupić, Miodrag Lazić, Slobodan Petrović, Milovan Purenović, Aleksandar Spasić, Dragoslav Stoiljković, Radmila Šećerov-Sokolović, Slobodan Šerbanović, Nikola Nikačević, Svetomir Milojević

Članovi uredništva iz inostranstva
Dragomir Bukur (SAD), Jiri Hanika (Češka Republika), Valerij Meshalkin (Rusija), Ljubiša Radović (SAD), Constantinos Vayenas (Grčka)

Likovno-grafičko rešenje naslovne strane
Milan Jovanović

Redakcija
11000 Beograd, Kneza Miloša 9/I
Tel/fax: 011/3240-018
E-pošta: shi@ache.org.rs
www.ache.org.rs

Izlazi kvartalno, rukopisi se ne vraćaju

Za izdavača: Ivana T. Drvenica

Sekretar redakcije: Ksenija Kostić

Izdavanje časopisa pomaže
Republika Srbija, Ministarstvo nauke, tehnološkog razvoja i inovacija

Uplata pretplate i oglasnog prostora vrši se na tekući račun Saveza hemijskih inženjera Srbije, Beograd, broj 205-2172-71, NLB Komercijalna banka a.d., Beograd

Menadžer časopisa i kompjuterska priprema
Aleksandar Dekanski

Štampa
Razvojno-istraživački centar grafičkog inženjerstva, Tehnološko-metalurški fakultet, Univerzitet u Beogradu, Karnegijeva 4, 11000 Beograd

Indeksiranje
Radovi koji se publikuju u časopisu *Hemijska Industrija* ideksiraju se preko *Web of Science (WoS)®* servisa *Science Citation Index - Expanded™* i *Journal Citation Report (JCR)*

SADRŽAJ/CONTENTS

Evaluation of a 3D osteosarcoma model: Experimental studies and mathematical modelling of drug response

Marija B. Pavlović[1], Ivana D. Banićević[1], Radmila M. Janković[2], Jasmina J. Stojkovska[1] and Bojana M. Obradović[1]

[1]*University of Belgrade, Faculty of Technology and Metallurgy, Belgrade, Serbia*
[2]*University of Belgrade, Faculty of Medicine, Belgrade, Serbia*

Abstract

Osteosarcoma remains a significant clinical challenge, with poor outcomes in metastatic cases and slow progress in the development of novel therapies. In this work, a previously developed 3D osteosarcoma model, comprising bone-mimicking macroporous alginate scaffolds with hydroxyapatite particles and a perfusion bioreactor, was evaluated as a tool for anticancer drug testing. Murine osteosarcoma cells (K7M2-wt) were seeded onto the scaffolds (15×10^6 cells *per* cm^3) and cultured statically for 1 day. In two experimental series, scaffolds were then exposed to doxorubicin (1 μg cm^{-3}) under perfusion for 1 or 3 days (40 μm s^{-1} superficial velocity), modelling post-resection conditions with predominantly individual or loosely aggregated cells. In two additional series, the same treatments were applied after 7 days of perfusion, when compact spheroids had formed, mimicking established tumours. Histological analysis and MTT assay were used to assess cell morphology and metabolic activity. Short-term treatment had negligible effects, while prolonged exposure significantly reduced metabolic activity of individual cells, but spheroid-like structures exhibited increased doxorubicin resistance. To rationalize the results from the first two series, a mathematical model was developed describing drug transport, intracellular accumulation, cell proliferation, and cell death. The model captured the initial treatment phase, but overestimated the effect of prolonged treatment, suggesting additional resistance mechanisms. Overall, the results demonstrate the potential of this 3D model for anticancer drug evaluation.

Keywords: K7M2-wt cell line; perfusion bioreactor; alginate scaffold; doxorubicin; anticancer drug testing; spheroids.

Available on-line at the Journal web address: http://www.ache.org.rs/HI/

ORIGINAL SCIENTIFIC PAPER

UDC 616-006.34:533.6.072 -023.5

Hem. Ind. **80(2)** 71-86 (2026)

1. INTRODUCTION

During past decades, the incidence of malignant bone tumours has shown a slight increase [1]. This is also the case for osteosarcoma, a primary malignant bone tumour that most commonly affects adolescents and young adults during the period of pubertal growth but also occurs in older patients [2] with an overall annual incidence of approximately 3.4 cases *per* million people [3]. The current way of treating osteosarcoma includes neoadjuvant chemotherapy followed by surgical resection of primary tumour and all clinically detected metastases. After surgery, adjuvant chemotherapy is given to eliminate any remaining cancer cells, which may persist and contribute to relapse and poor clinical outcomes. Chemotherapy is administered in multiple cycles with chemotherapeutic drugs given over one or several consecutive days, followed by a recovery period before the next cycle [3]. The drugs currently in use have remained largely unchanged for 30 to 40 years and attempts to optimize standard therapy over the past 20 years have not yielded significant improvements [4]. Therefore, there is a strong need for the development of new therapies, particularly for patients diagnosed with metastases and those experiencing relapse. However, the validation of new drugs is a time-consuming process, and many potential drug candidates fail in clinical trials, often due to the limitations of experimental

Corresponding authors: Jasmina J. Stojkovska, E-mail: jstojkovska@tmf.bg.ac.rs https://orcid.org/0000-0002-6732-3037 Faculty of Technology and Metallurgy, University of Belgrade, Belgrade, Serbia and Bojana M. Obradović E-mail: bojana@tmf.bg.ac.rs https://orcid.org/0000-0002-7276-0442 Faculty of Technology and Metallurgy, University of Belgrade, Belgrade, Serbia
Co-authors: Marija B. Pavlović https://orcid.org/0009-0004-3055-7413, Ivana D. Banićević https://orcid.org/0000-0003-1494-3264 and Radmila M. Janković https://orcid.org/0000-0001-5733-9505

Paper received: 6 July 2026; Paper accepted: 10 September 2026; Paper published: xx September 2026.
https://doi.org/10.2298/HEMIND260706008P

preclinical models [5]. Among these, animal testing and cell cultures grown in a monolayer (two-dimensional (2D) cell cultures) are still widely used in preclinical research and can provide valuable insights into drug response. However, animal testing can be very costly, raises ethical concerns, and the results are not always reproducible or reliably translatable to humans [6]. In contrast, 2D cell cultures enable rapid, simple, and highly reproducible testing; however, they do not faithfully represent the complex *in vivo* environment in which osteosarcoma develops and progresses. Three-dimensional (3D) osteosarcoma cell culture models offer an additional level of complexity and can more closely mimic the *in vivo* tumour environment, including cell-cell and cell–microenvironment interactions, thereby enabling a more comprehensive evaluation of anticancer drug efficacy [7]. For example, 3D multicellular tumour spheroids, which are aggregates formed by cancer cells, represent a relatively simple model in which cells secrete extracellular matrix (ECM) and exhibit behaviour similar to that observed *in vivo* [8]. They can be cultured under static conditions or, for improved mass transport, in microfluidic devices and biomimetic bioreactors [9]. Furthermore, to better mimic the tissue ECM, spheroids can be directly encapsulated within biomaterial scaffolds, or individual cells can be seeded onto scaffolds and allowed to subsequently form aggregates. Scaffolds for osteosarcoma models aim to imitate the structure and composition of bone tissue ECM, which consists of an organic phase (predominantly collagen) and a mineral, inorganic phase (predominantly hydroxyapatite). Accordingly, composite scaffolds combining polymers and mineral particles offer an attractive approach for 3D cell cultures, as demonstrated by alginate-calcium phosphate scaffolds, which supported osteosarcoma cell growth [10]. In addition to having a suitable composition, scaffolds are typically highly porous with interconnected pores of at least 100 μm in diameter, to enable effective osteosarcoma cell adhesion and efficient nutrient transport, thereby supporting cell survival and function [11-13]. Mass transport within such scaffolds can be enhanced using perfusion bioreactors that provide also relevant hydrodynamic shear stresses [14,15]. It has been shown that perfusion can efficiently mimic functional features observed *in vivo*, promote cell aggregation and spheroid formation, and thereby contribute to the development of a more physiologically relevant tumour model, supporting reliable testing of anticancer compounds [16,17].

3D models are also powerful tools for quantitatively analysing experimental results through the mathematical modelling, particularly in relating anticancer drug transport and cellular responses [18]. A comprehensive understanding of pharmacokinetic and pharmacodynamic processes is crucial for linking drug exposure to these responses [19]. However, establishing a quantitative relationship remains challenging, as cytotoxic effects often occur with a delay and involve complex intracellular cascades that are difficult to capture with simple models [20,21]. To address these challenges, various modelling approaches have been proposed. Some models assume that cell death is directly related to extracellular drug concentration, while others relate it to the area under the concentration-time curve (AUC) or use a Hill-type dependence [19]. In contrast, Eliaz and coworkers assumed that the cytotoxic potency of a drug is a function of the intracellular drug amount in a critical cellular compartment, rather than the drug concentration in the surrounding medium. In this model, cell death begins after a lag phase, as observed experimentally, and the total number of viable cells at any given time is determined by the balance between cell proliferation and drug-induced cell death [22]. However, these studies were performed in cell monolayers, while relatively few studies focus on more relevant 3D systems integrating drug transport, intracellular accumulation, and cellular response.

The aim of the present study was to investigate the potential of a previously developed 3D osteosarcoma cell culture model based on the use of macroporous composite alginate hydrogel with mineral particles as a cell carrier in a perfusion bioreactor, for assessing the effects of anticancer drugs [10]. In the present work, hydroxyapatite particles were used as a mineral phase, while doxorubicin was selected as a model drug. Specifically, the drug was applied both to scaffolds immediately after cell seeding and to cultured cell-seeded scaffolds after spheroid-like structures had formed. This approach allowed us to evaluate the effects of doxorubicin on individual and loosely aggregated cells simulating the post-surgical scenario with residual cancer cells, as well as on spheroid-like structures formed during perfusion culture, representing neoadjuvant chemotherapy conditions. Four experimental series were performed, in which doxorubicin was used at a concentration and treatment regime relevant for clinical application (1- and 3-day exposure). Finally, to rationalize the experimental results, an attempt was made to develop and apply a mathematical model describing doxorubicin transport, intracellular accumulation, and cell proliferation and death within the perfused scaffolds based on the model proposed in literature [22].

1. MATERIALS AND METHODS

2. 1. Materials

For the preparation of macroporous scaffolds, low-viscosity sodium alginate (A3249) was purchased from AppliChem (Germany), hydroxyapatite (HAp; particle size 2.5 μm, surface area ≥ 80 m^2 g^{-1}) and calcium chloride dihydrate ($CaCl_2 \cdot 2H_2O$) were obtained from Sigma-Aldrich (USA), isopropanol was purchased from Zorka Pharma (Serbia), and disodium ethylenediaminetetraacetate dihydrate (Na_2-EDTA$\cdot 2H_2O$) was supplied by HiMedia Laboratories Pvt. Ltd. (India). High glucose Dulbecco's Modified Eagle's medium with L-glutamine (DMEM) was obtained from Biological Industries (Israel), fetal bovine serum (FBS) from Gibco (Brazil) and penicillin/streptomycin solution from Sigma-Aldrich (Israel). Phosphate-buffered saline (PBS), trypan blue solution and trypsin-EDTA solution were obtained from Sigma-Aldrich (USA) and doxorubicin from Ebewe (Austria). MTT solution (3-(4,5-dimethylthiazol-2-yl)-2,5-dyphenyl tetrazolium bromide) was purchased from Sigma (USA), dimethyl sulfoxide (DMSO) from Fisher Scientific (UK), formaldehyde solution (35–37%) from NRK Inženjering (Serbia) and hematoxylin-eosin (H&E) staining solution from BioGnost (Croatia).

2. 2. Cell culture

Murine osteosarcoma cells K7M2-wt (ATCC® CRL-2836™, USA) were cultured in T-flasks in complete culture medium (cDMEM), containing DMEM, 10% fetal bovine serum and 1% penicillin-streptomycin solution under standard conditions (37 °C, 5% CO_2 in a humidified atmosphere). When the confluence of about 80-90% was reached, the cells were detached by using trypsin /EDTA solution. Briefly, the attached cells in T-flasks were washed twice with 5 cm^3 PBS and treated with 1 cm^3 of trypsin/EDTA solution for 5 min at 37 °C, which was then neutralized with cDMEM. The resulting cell suspension was collected, transferred to a centrifuge tube, and centrifuged at 1200 rpm for 5 min to obtain a cell pellet. The pellet was then resuspended and used for cell counting and preparation of the cell suspension for seeding.

2.3. Production of macroporous composite alginate scaffolds

Macroporous composite alginate scaffolds were produced according to a previously established procedure [23]. Hydroxyapatite powder (HAp) was dispersed in a 0.33 wt.% $CaCl_2 \cdot 2H_2O$ solution using an ultrasonic probe (750 W, 30 s). The obtained dispersion (10 wt.% HAp; 0.30 wt.% $CaCl_2 \cdot 2H_2O$) was mixed with 2.5 wt.% Na-alginate solution under intensive stirring to avoid early gelation, resulting in a final mixture containing 2 wt.% Na-alginate, 2 wt.% HAp, and 0.06 wt.% $CaCl_2 \cdot 2H_2O$. The mixture was poured into a previously activated dialysis tubing (2.5 cm in diameter, 15 cm in length), activated by boiling in 10 mM Na_2-EDTA$\cdot 2H_2O$ for 30 min and subsequently immersed in 3.97 wt.% $CaCl_2 \cdot 2H_2O$ solution under slow stirring for 24 h. Following replacement with a fresh solution, incubation continued for another 24 h to ensure complete gelation. The obtained composite cylinders were then rinsed with distilled water, dried, placed in a freezing container filled with isopropanol and frozen overnight at a controlled rate down to −70 °C. The frozen samples were lyophilized (−70 °C, 0.011 mbar, 24 h) in a freeze-dryer (Beta 2-8 LDplus, Martin Christ Gefriertrocknungsanlagen GmbH, Germany) and then sterilized by UV irradiation for 30 min.

2. 4. Cell seeding

Prior to cell seeding, the obtained dry composite cylinders were immersed in complete cell culture medium and incubated for 1 h. After incubation, the cylinders were cut into disc-shaped scaffolds approximately 4.5 mm thick, which were then placed in 24 well plates, covered with 125 mm^3 of complete culture medium, each, and left in an incubator for 3 h. After the rehydration, the dimensions of each scaffold were measured using a vernier caliper. The final scaffolds had an average diameter of 9.0 ± 0.3 mm and average thickness of 4.4 ± 0.4 mm (determined for n = 18). For cell seeding, each scaffold was placed in a well of non-adherent 12-well plates and the cell suspension (167×10^6 cells *per* cm^3) was poured onto the upper scaffold surface (42.6 ± 5.4 mm^3), so to obtain a nominal cell density of 15×10^6 cells *per* cm^3 of scaffold volume. The plates were then placed in the incubator for 1 h, after which 2.5 cm^3 of complete medium was added to each well to fully submerge the scaffolds. The scaffolds were then incubated at 37 °C in a humidified atmosphere containing 5 % CO_2 and cultured for 24 h to ensure initial cell adhesion and adjustment to the scaffolds.

Cell seeding efficiency (*E*) was calculated as the difference between the initial number of cells in the suspension and the number remaining in the medium 24 h after seeding, divided by the initial cell number. Cell numbers were determined by the trypan blue exclusion method using a hemocytometer and an inverted optical microscope Olympus CKX53 (Olympus, Japan). It should be noted that this calculation assumes negligible cell proliferation in the medium or on the well bottom during the initial 24 h of static culture, which may not be entirely accurate. Therefore, the actual seeding efficiencies may be somewhat higher than the calculated values.

2. 5. Perfusion bioreactor culture and doxorubicin treatment

In all experiments, following the initial 24 h static culture, perfusion cultures were established in "3D Perfuse" perfusion bioreactor systems (Innovation Center of the Faculty of Technology and Metallurgy, University of Belgrade, Serbia) (Figure 1a). In brief, each cell-seeded scaffold was placed in a separate bioreactor chamber formed by a piece of silicone tubing (12 mm in diameter, 30 mm in length) and each bioreactor chamber was then connected to a separate recirculation loop including a medium reservoir, silicone tubing for medium recirculation and gas exchange, as well as two syringes for medium exchange. Each system was filled with 15 cm³ of cDMEM and placed in a humidified incubator (37 °C, 5% CO_2). In all experiments, the systems were continuously perfused by a multichannel peristaltic pump (Shenzhen, China) at a flow rate of 0.27 cm³ min^{-1} corresponding to the superficial velocity of 40 μm s^{-1}. Four experimental series were performed in which doxorubicin was added to the medium in the reservoir at a concentration of 1 μg cm^{-3}. In the first two experimental series the treatment started immediately after the systems were established and lasted for one and three days, respectively, in order to assess the drug effects on individual and loosely aggregated osteosarcoma cells. In the remaining studies, the cell-seeded scaffolds were cultured under continuous medium perfusion for 7 days to allow for the spontaneous formation of spheroid-like structures, after which they were treated with doxorubicin for one and three days. In the case of the three-day treatments, the treatment medium was completely replaced daily with a fresh dose of doxorubicin added to the reservoir. In all experiments, untreated perfused cultures served as controls. For each experimental group, at least two scaffolds (and in some cases three) were used in each experiment. All experiments involving three-day treatments of individual and loosely aggregated cells, and spheroid-like cultures were independently repeated twice.

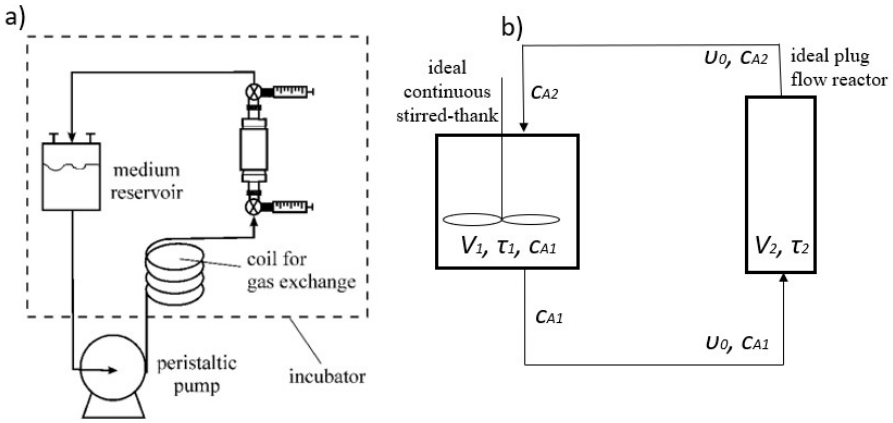

Figure 1. *Perfusion bioreactor system consisting of a bioreactor chamber, tubing for medium recirculation, a medium reservoir, and a peristaltic pump that provides continuous medium flow: a) schematic presentation of the experimental system (modified with permission from [24]); b) model of the system consisting of a plug flow reactor with volume V_2 and residence time τ_2, and an ideally stirred vessel with volume V_1 and residence time τ_1; υ_0 represents the volumetric flow rate through the system, while c_{A1} and c_{A2} are the doxorubicin concentrations in the vessel (and at the reactor inlet) and at the reactor outlet, respectively*

2. 6. Analytical methods

2. 6. 1. MTT assay

The MTT assay was used before and after bioreactor cultures to assess the cell metabolic activity within the scaffolds. An MTT stock solution (5 mg cm^{-3} in PBS) was diluted with cDMEM to a final concentration of 0.5 mg cm^{-3}. One scaffold or a half of a scaffold was covered with 2 cm³ of MTT solution (0.5 mg cm^{-3}) and incubated for 3.5 h at 37 °C. After

incubation, the scaffolds were cut in small pieces, and the formed formazan crystals were dissolved in 4 to 7 cm³ DMSO using an optimized sequential procedure (sequential additions of 1 to 1.5 cm³ every 20 min). After each extraction, the DMSO was collected separately and replaced with fresh DMSO; finally, the absorbance was measured in the combined collected solutions at 570 nm using a UV-1800 spectrophotometer (Shimadzu, Japan), with DMSO as the blank.

2. 6. 2. Histological analyses

After removal from the bioreactor chambers, the scaffolds (either entire or halves) were immersed in 4 % pH-neutral buffered formaldehyde (10 % formalin) for at least 24 h followed by dehydration through a graded series of ethanol solutions (70, 96 and 100 %), clearing in xylene, and embedding in paraplast (Sakura Tissue-Tek TEC, CA, USA). The embedded scaffolds were sectioned using a microtome (Leica Reinhart, Austria; Leica SM 2000 R, Germany) to obtain 5 µm-thick cross-sections, which were then stained with H&E [25]. Formed spheroid-like structures were analysed by scanning the cross-sections using an Olympus DP70 camera connected to a light microscope (Olympus BX51, Japan) and evaluated for the number as well as the size and shape using AperioImageScope (Leica Biosystems Imaging, Inc., USA, https://www.leicabiosystems.com/digital-pathology/manage/aperio-imagescope/) and ImageJ software (https://imagej.net/ij/) respectively.

2. 6. 3. Statistical analysis

Data were analysed using one-way ANOVA, followed by Welch's two-sample t-tests for comparisons between groups (two-tailed) using Microsoft Excel software (Microsoft Corp., USA). All quantitative data are expressed as a mean ± standard deviation. Statistical significance is accepted as p <0.05.

2. 7. Mathematical modelling of doxorubicin transport and effects on cells

A mathematical model of doxorubicin transport and accumulation in cells coupled with cell proliferation and death was derived with the aim to quantify the effect of doxorubicin treatment on individual cells in the 3D osteosarcoma cell culture model. The case of a 3-day doxorubicin treatment was modelled, in which the medium was replaced, and a fresh dose of doxorubicin was added at the beginning of each day. The experimental recirculation system (Figure 1a) was modelled as a plug flow reactor connected with an ideally stirred vessel (Figure 1b). During each pass through the scaffold, represented by the reactor, doxorubicin is taken up by the cells, resulting in a decrease in drug concentration in the medium. The medium then enters the vessel, where perfect mixing is assumed, before returning to the scaffold.

The scaffold is represented as a plug flow reactor with a volume corresponding to the void volume of the scaffold pores. The doxorubicin concentration (c_A) decreases along the reactor length due to cellular accumulation at a rate ($-r_A$), yielding Equation (1):

$$-\mathrm{d}c_A = -r_A \, d\tau_2 \tag{1}$$

where τ_2 is the reactor residence time. Accumulation of doxorubicin in cells was assumed to follow the first-order kinetics, Equation (2) based on the experimental data in literature [22]:

$$-\frac{\mathrm{d}n_A}{\mathrm{d}t} = kc_A N_{cell} \tag{2}$$

where n_A is the total intracellular amount of doxorubicin accumulated in all cells, k is the uptake rate constant and N_{cell} is the total number of cells. Dividing Equation (2) by the volume of the plug flow reactor (V_2) yields an expression for the accumulation rate ($-r_A$), which can be then substituted into Equation (1) to provide a differential Equation (3):

$$-\frac{\mathrm{d}c_A}{c_A} = \frac{kN_{cell}}{V_2}\mathrm{d}\,\tau_2 \tag{3}$$

Integration of Equation (3) provides the change in drug concentration during a single pass through the scaffold, Equation (4):

$$c_{A2} = c_{A1} e^{\frac{-kN_{cell}\tau_2}{V_2}} \tag{4}$$

where c_{A1} and c_{A2} represent the doxorubicin concentration in the medium at the reactor inlet and the outlet, respectively.

In the reservoir, the medium is perfectly mixed, resulting in a governing equation for the change in doxorubicin concentration, Equation (5):

$$\left(c_{A2}\text{-}c_{A2}\right)=\frac{\mathrm{d}c_{A1}}{\mathrm{d}\tau}\tau_1 \tag{5}$$

where τ_1 is the residence time of medium in the reservoir (including the tubing volume). The total number of viable cells in the scaffold depends on time (τ) and is determined by the balance between the rates of cell proliferation and cell death induced by doxorubicin accumulation described by differential Equation (6) [22]:

$$\frac{\mathrm{d}N_{\mathrm{cell}}}{N_{\mathrm{cell}}}=\left(k_s\text{-}k_u nA_{\mathrm{Ai}}\right)\mathrm{d}\tau \tag{6}$$

where k_s is the rate constant of cell proliferation, k_u is the rate constant of cell death, and n_{Ai} is the intracellular amount of doxorubicin per cell. However, according to literature [22], a lag time of 3 hours was assumed, during which the cells proliferate and the intracellular amount of doxorubicin increases without any apparent effect. Thus, during this period, Equation (6) reduces to Equation (7):

$$\frac{\mathrm{d}N_{\mathrm{cell}}}{N_{\mathrm{cell}}}=k_s\mathrm{d}\tau \tag{7}$$

Change in the total intracellular amount of doxorubicin accumulated in all cells within a scaffold (n_{A}) over time is calculated from the mass balance of doxorubicin in the reactor, as given by Equation (8):

$$\left(c_{A1}\text{-}c_{A2}\right)\nu_0=\frac{\mathrm{d}n_{\mathrm{A}}}{\mathrm{d}\tau} \tag{8}$$

where ν_0 is the medium flow rate. The amount of drug per cell is then obtained by dividing this value by the total number of viable cells in the scaffold and adding it to the previously accumulated intracellular amount ($n_{\mathrm{Ai,prev}}$), as described by Equation (9):

$$n_{\mathrm{Ai}}=\frac{\mathrm{d}n_{\mathrm{A}}}{N_{\mathrm{cell}}}+n_{\mathrm{Ai,prev}} \tag{9}$$

The resulting system of ordinary differential equations was solved numerically in Python using the Runge-Kutta method [26]. The procedure started by solving Equation (5) for one pass through the reactor, lasting τ_2. The amount of doxorubicin consumed during that pass was calculated by Equation (8) and the resulting internal doxorubicin amount per cell was determined by Equation (9). The number of viable cells was then calculated using Equation (7) for the first 3 hours, and Equation (6) thereafter. Finally, the new doxorubicin concentration c_{A1} after passing through the reservoir was calculated using Equation (5) and the entire calculation process was repeated for each subsequent pass through the reactor (*i.e.,* scaffold).

3. RESULTS

In this study, a previously developed 3D osteosarcoma cell culture model based on macroporous composite alginate/HAp scaffolds and perfusion bioreactor, was evaluated for anticancer drug testing with doxorubicin selected as a representative drug. Similarly, to the previous study [10], osteosarcoma cells were successfully seeded onto the scaffolds achieving a high seeding efficiency of about 86±8 %. As previously reported, after 1 day of static culture, individual cells and loose aggregates could be observed, which further formed denser, spheroid-like structures over 7 days of cultivation under medium perfusion. This establishes a robust model system for studying the effects of doxorubicin on both individual cancer cells and more mature, tumour-like aggregates. Accordingly, four experimental series were performed with doxorubicin applied at a concentration of 1 μg cm $^{-3}$, a dosage commonly used in studies of its effects on osteosarcoma cells [27-28]. The treatment regimens, lasting either 1 or 3 days, were inspired by clinically relevant protocols. In the first two experimental series, doxorubicin was applied immediately after establishing the bioreactor culture (*i.e.* one day after cell seeding and static culture) to examine its effects on individual cells. In the third and fourth series, the treatment began after 7 days of bioreactor culture to assess the effects on spheroid-like structures.

3. 1. Effects on individual and loosely aggregated cells

In the first two experimental series doxorubicin was applied for 1 and 3 days upon the set-up of perfusion cultures, respectively, and the resulting cultured scaffolds were examined for cell metabolic activity by the MTT assay and morphological appearance by histological analyses. Untreated cultures served as controls in both cases. The MTT assay showed that the cell metabolic activity in the initial scaffolds (n = 7) in both experimental series was similar, as the absorbance values of the dissolved formazan solutions were not statistically different; therefore, these initial control values are presented as a single average. However, absorbance values from cultured scaffolds were normalized to their respective initial scaffolds (Figure 2).

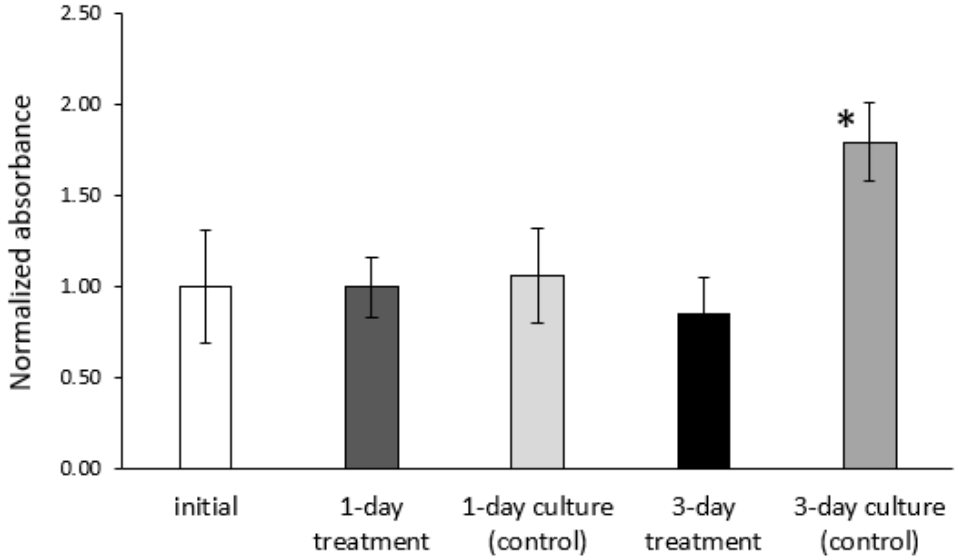

Figure 2. *Absorbance values normalized to the corresponding values determined for initial scaffolds cultured statically for 24 h after seeding, shown for initial scaffolds (n = 7), scaffolds treated with doxorubicin for one day (n = 3), scaffolds treated with doxorubicin for three days (n = 5), and respective untreated control scaffolds (n = 2 and n = 4, respectively) (*indicates a statistically significant difference between the 3-day control group and each of the other groups: 3-day treatment, 1-day treatment, and initial scaffolds)*

The results shown in Figure 2 demonstrate that the 1-day treatment did not induce any adverse effect on the cell metabolic activity. In contrast, following the 3-day treatment, the metabolic activity remained similar to that of the initial scaffolds, while the untreated control exhibited approximately a twofold increase in metabolic activity over the 3-day perfusion culture.

Figures 3 and 4 show H&E-stained histological cross-sections of doxorubicin-treated scaffolds for 1 and 3 days, respectively, and corresponding untreated controls. Individual cells (indicated by black stars) and loose cell aggregates (indicated by black arrows) are clearly visible within the pores of control scaffolds as well as scaffolds treated with doxorubicin for one day. The alginate matrix appears light purple, while hydroxyapatite particles are seen as dark-purple spots. Histological analysis was consistent with the results obtained by the MTT assay. In specific, when comparing the controls after 1 and 3 days of perfusion culture, apparently a higher number of denser aggregates, along with individual cells, were observed in the latter culture (Figs 3b and 4b, respectively). A 1-day doxorubicin treatment did not induce any visible effect, as the histological cross-sections of treated and control scaffolds appeared similar (Figure 3). In contrast, after 3 days of treatment, individual cells could rarely be observed, with mostly relatively dense aggregates remaining (indicated by black triangles) (Figure 4a). These results demonstrate that the 3-day treatment was effective against cells directly exposed to the drug, whereas cells within compact spheroid structures were less affected, likely due to the protective effects of three-dimensional cellular organization and possibly reduced drug diffusion into the spheroid interior.

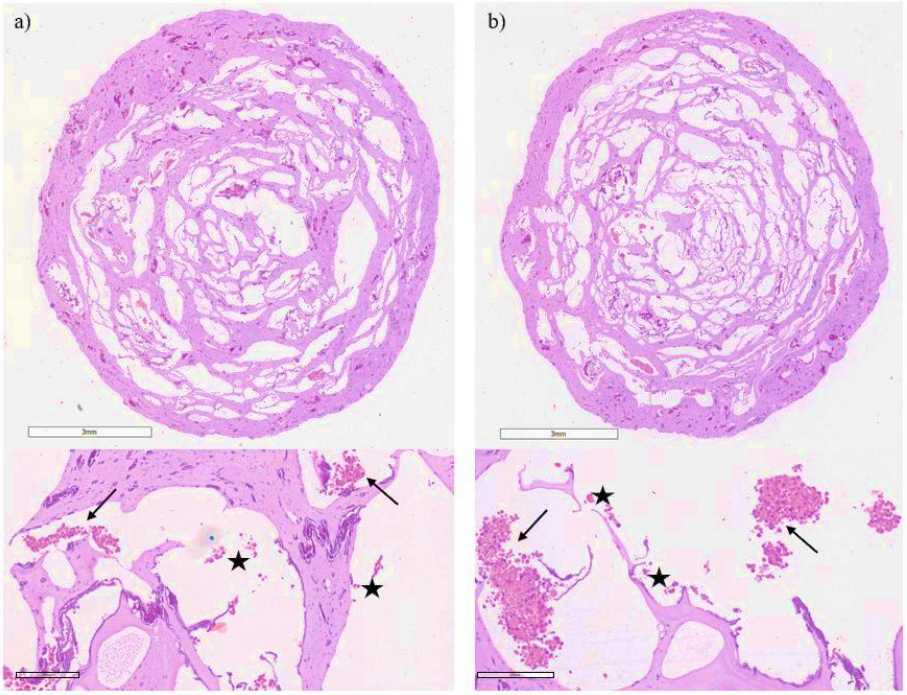

Figure 3. *Histological cross-sections of scaffolds after 1-day perfusion culture: a) treated with doxorubicin; b) control (untreated); black stars indicate individual cells, while arrows mark regions with loosely aggregated cells (upper panels: entire cross-sections: scale bar = 3 mm; lower panels: representative regions at higher magnification, scale bar = 200 µm; H&E stain)*

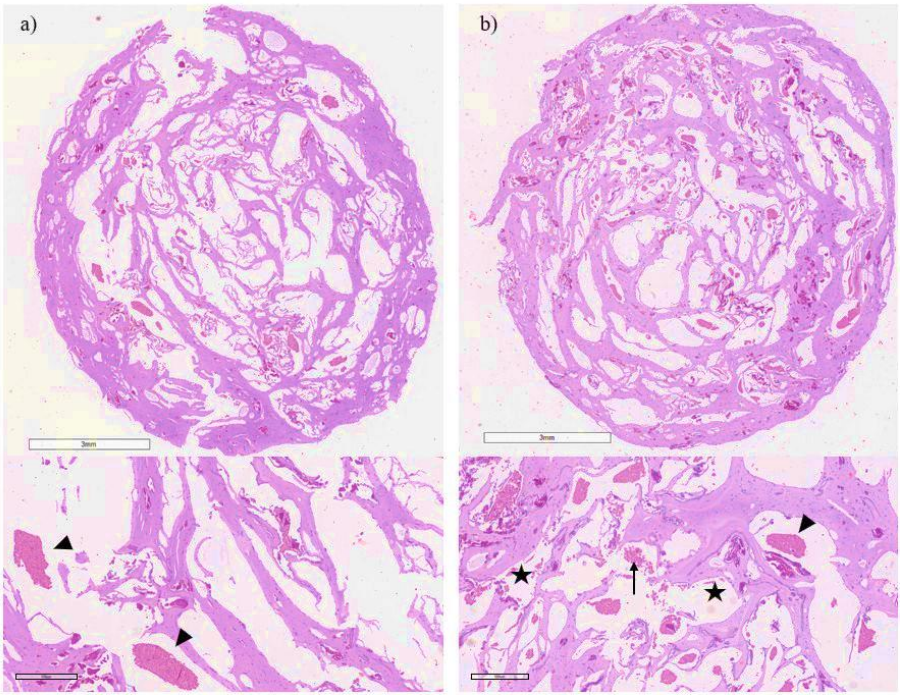

Figure 4. Histological cross-sections of scaffolds after 3-day perfusion culture: a) treated with doxorubicin; b) control (untreated); triangles indicate spheroid-like structures, black stars indicate individual cells, and arrows mark regions with loosely aggregated cells (upper panels: entire cross-sections: scale bar=3 mm; lower panels: representative regions at higher magnification, scale bar=500 µm; H&E stain)

3. 2. Effects on spheroid-like structures

The third and fourth experimental series aimed to evaluate the effectiveness of 1- and 3-day doxorubicin treatments (1 µg cm^{-3}), respectively, on compact spheroid structures formed after 7 days of perfusion culture. The 1-day treatment

did not affect either the metabolic activity or the morphological appearance of the cell spheroids, as shown by the MTT assay and histological analysis of all samples (Supplementary material, Figures S1 and S2, respectively). These findings indicate that this exposure time was insufficient to inhibit cell activity within spheroid structures similarly to the results of 1-day treatment of the initial scaffolds.

In contrast, the 3-day treatment produced some effects on the cells, as indicated by the MTT assay, which showed a slightly lower, though not statistically significant, metabolic activity in the treated samples compared to the untreated controls (Figure 5). High standard deviations in all results should be noted.

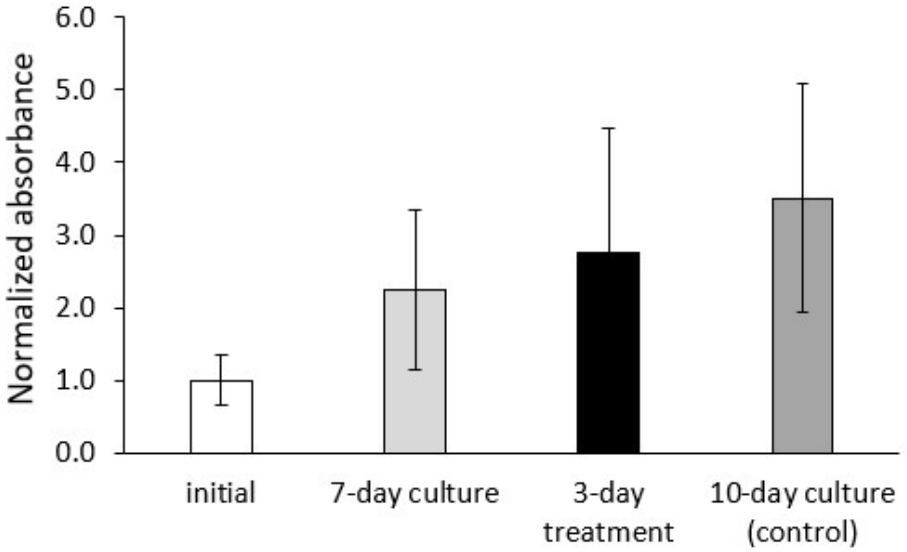

Figure 5. *Absorbance values normalized to the initial scaffolds cultured statically for 24 h after seeding, shown for: initial scaffolds (n = 3), scaffolds after 7 days of perfusion (n = 4), scaffolds treated with doxorubicin for 3 days following 7 days of perfusion (n = 5), and control scaffolds cultured under perfusion for 10 days (n = 4)*

Histological cross-sections of scaffolds before the doxorubicin treatment (*i.e.* after one day of static culture followed by 7-day perfusion, Figure 6a) show only compact spheroid-like aggregates within the scaffolds. This indicates that, during this cultivation period, the loosely aggregated and individual cells, clearly visible in control samples at earlier time points (Figures 3 and 4) underwent self-organization and extracellular matrix production, resulting in formation of dense spheroid-like structures.

Viable, compact spheroid-like structures with apparently the same morphology are also visible in scaffolds that underwent a 3-day doxorubicin treatment, as well as in the controls cultured for 10 days under perfusion in total (Figures 6b and 6c, respectively). However, due to the random distribution of spheroids and the variability introduced by random sectioning planes, it was not feasible to perform thorough statistical analyses of spheroid number and size across different groups within the scope of this study.

3. 3. Mathematical modelling of doxorubicin transport and effects on cells

To quantify the effects observed in the 3-day doxorubicin treatment of initial scaffolds a mathematical model was derived to describe the doxorubicin transport within the recirculating perfusion bioreactor system, intracellular drug accumulation, and the resulting change in the cell number over time. Model parameters were adopted based on the values obtained from the present experiments and data taken from literature (Table 1). In specific, the initial doxorubicin concentration used in the model corresponded to that applied experimentally (c_A = 1.84 μmol dm^{-3}). The initial number of cells (N_{cell}) was estimated as the average seeding value multiplied by the average seeding efficiency, as determined experimentally, resulting in 3,648,375 cells per scaffold. The plug flow reactor volume (V_2) was calculated as the total pore volume in the scaffold, based on a measured porosity of approximately 40 % from scaffold cross-sections. The reservoir volume V_1 corresponding to the medium volume in the system loop was calculated as a difference between the total medium volume added to the system and the scaffold pore volume.

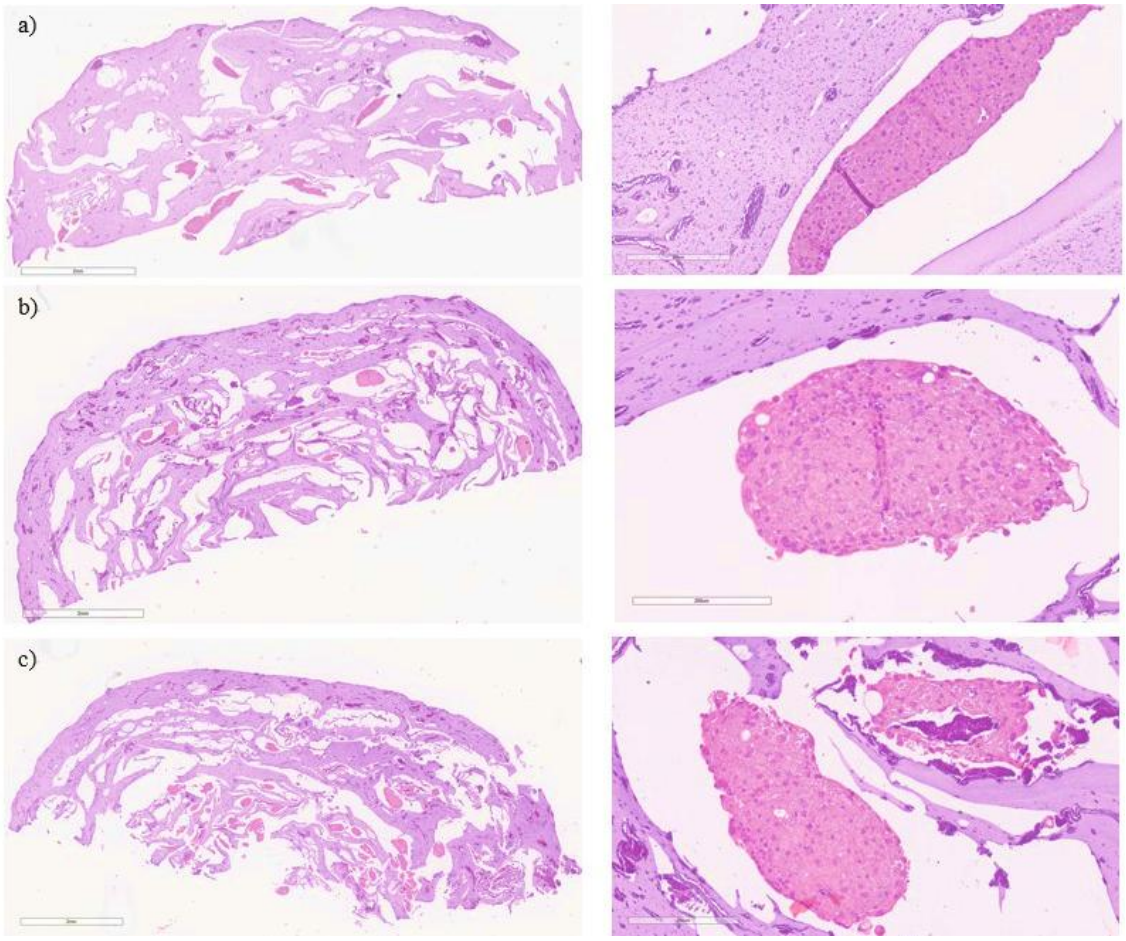

Figure 6. *Histological cross-sections of scaffolds: a) cultured under bioreactor conditions for 7 days; b) cultured under bioreactor conditions for 7 days and then treated with doxorubicin for three days; (c) control (untreated) scaffold cultured under bioreactor conditions for a total of 10 days (left panels: half cross-sections, scale bar = 3 mm; right panels: representative regions at higher magnification, scale bar = 200 μm; H&E stain)*

The medium flow rate was 0.27 $cm^3\ min^{-1}$. The remaining model parameters were derived or adopted from literature data. The uptake rate constant k was calculated using Equation (3) based on experimental data reported in literature [22] for B16F10 melanoma cells treated with doxorubicin within a concentration range that includes the value used in the present study, 1.84 μmol dm^{-3} (Supplementary material, Figure S3). The cell death rate constant, k_u, was adopted from literature as 1.04×10^{11} $(mol\ min)^{-1}$ [22]. The cell proliferation rate constant, k_s, was determined 3.73×10^{-4} min^{-1} from the cell doubling time provided in the ATCC product datasheet for the K7M2-wt cell line.

Table 1. *Parameters used in the mathematical model*

Parameter	Value
N_{cell}	3,648,375
c_A / μmol dm^{-3}	1.84
V_1 /cm^3	14.887
V_2 / cm^3	0.11286
ν_0 / $cm^3\ min^{-1}$	0.27
τ_1 /min	55.14
τ_2 / min	0.42
k / $dm^3\ min^{-1}\ cell^{-1}$	3.68×10^{-12}
k_u / $mol^{-1}\ min^{-1}$	1.04×10^{11}
k_s / min^{-1}	3.73×10^{-4}

The system of ordinary differential equation was solved as described in section 2.7. with time intervals equal to the bioreactor residence time τ_2 = 0.42 min. The simulation provides time-dependent profiles of drug concentration,

intracellular drug accumulation, and changes in the cell number over time. During the first 24 h of treatment the model predicts a gradual decline in doxorubicin concentration in the medium due to continuous accumulation of the drug in the cells during repeated passes through the scaffold (Figure 7a). At the same time, the intracellular amount of doxorubicin per cell increases, reaching 1.1 fmol *per* cell after 180 min (Figure 7b), which is comparable to the 1.2 fmol reported by Eliaz *et al.* [22] for the same initial timeframe. According to the authors and as adopted in the model, only cell proliferation occurs during this time, resulting in a gradual increase in cell number. After this period, drug induced cell death is included in the model; however, the overall cell population remains nearly constant during the first day of exposure, with the model predicting an overall increase in the viable cell number of only 7 % (Figure 7c). This result is consistent with the experimental MTT analysis results, which showed negligible differences in metabolic activity before and after the treatment in the first experimental series (Figure 2).

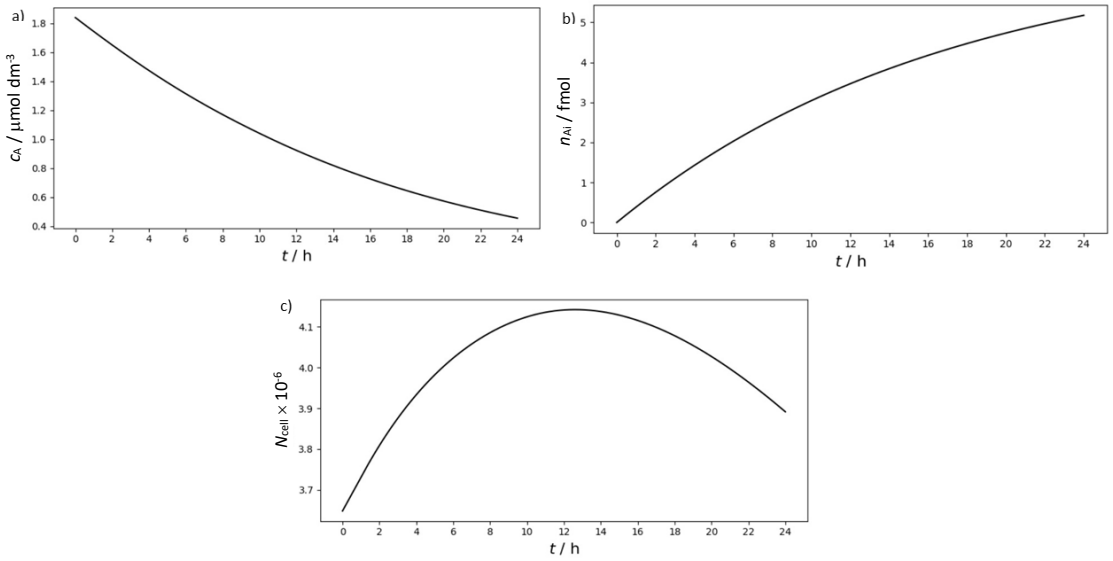

Figure 7. *Predicted profiles of: a) drug concentration in the medium, b) intracellular drug accumulation and c) viable cell number during the first day of the doxorubicin treatment*

On the second day, the medium is replaced and a fresh dose of doxorubicin is added, and this procedure is then repeated on the third day. Doxorubicin concentration profiles for all 3 days are shown in Figure 8.

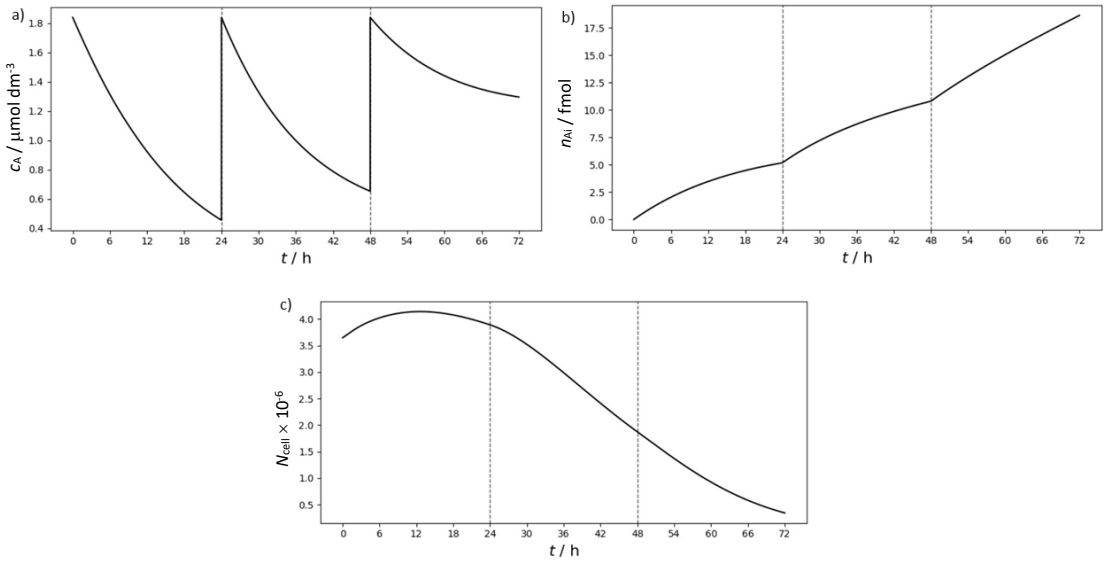

Figure 8. *Predicted profiles of: a) drug concentration in the medium, b) intracellular drug accumulation and c) viable cell number during the 3 days of doxorubicin treatment*

Each subsequent dose of doxorubicin is distributed among fewer cells, whereas the intracellular amount of accumulated doxorubicin continues to increase. Consequently, the cell death rate increases, resulting in a progressively faster decline in the cell population. By the end of the third day, the model predicts approximately 3.4×10^5 remaining cells or approximately 9 % of the initial cell population. However, this prediction is not consistent with the experimental results. The MTT assay demonstrated only an approximately 15 % decrease in metabolic activity after the 3-day treatment (Figure 2), suggesting that the model overestimated the effect of doxorubicin. Histological cross-sections also confirmed the presence of viable cells after the treatment although mostly in dense aggregates (Figure 4a).

4. DISCUSSION

The present study builds on a previously developed 3D osteosarcoma cell culture model based on macroporous composite alginate scaffolds with mineral particles and a biomimetic perfusion bioreactor, with the modification that the mineral component in this work consists only of hydroxyapatite [10]. As previously confirmed, this model provides a suitable environment for bone cancer cell cultivation without negative effects on the cells, supporting cell growth and proliferation under bone tissue-like conditions. Individual and loosely aggregated cells observed after one day of initial static culture, progressively formed more compact, spheroid-like structures during 7 days of cultivation under continuous medium flow (0.27 cm^3 min^{-1}; superficial velocity of 40 µm s^{-1}) (Figure 6). This structural evolution enables the establishment of a robust model system for studying the effects of anticancer drugs on both individual cancer cells and more mature, spheroid-like structures. Doxorubicin was selected as a representative chemotherapeutic and applied at 1 µg cm^{-3} for one and three days. The results showed that the 1-day treatment was not effective for either individual and loosely aggregated cells or compact spheroid-like structures (Figures 2 and S1). The observed lack of effect is consistent with previous studies on 3D tumour spheroids, including U2OS osteosarcoma spheroids, which showed that metabolic activity did not significantly change across all tested doxorubicin concentrations (10, 20, 30 and 40 µM) compared to untreated controls [8]. In those studies, significant inhibition was observed only after 3 to 5 days of exposure**.** In comparison, the concentration used in the present study (~1.84 µM) is substantially lower, which may contribute to the negligible effect observed after one day of treatment.

A 3-day drug treatment, inspired by clinically relevant exposure protocols [3] was effective in the case of individual and loosely aggregated cells, as confirmed by the MTT assay (Figure 2), which showed reduced metabolic activity in treated samples. In addition, histological analysis revealed that individual cells were rarely observed, with mostly relatively dense aggregates remaining (Figure 4). The same treatment applied to compact spheroid-like structures formed during preceding seven days of bioreactor cultivation did not induce any significant effect although treated samples showed a slight trend toward reduced metabolic activity and a slight increase in the fraction of smaller spheroids (Figure 5). Similar findings were reported in a study using a 3D perfused tumour spheroid model, where 5-fluorouracil treatment (1 µg cm^{-3}) for 48 and 96 h did not significantly reduce the cell number or tumour volume. In contrast, in 2D cultures, cell number decreased by about 50 % after 48 or 96 h of exposure [16]. Also, in osteosarcoma models using the MG-63 bone cancer cell line cultured under perfusion conditions, liposomal doxorubicin at concentrations equivalent to the 2D IC_{50} (~0.1 µg cm^{-3}) exhibited minimal cytotoxic effects, even after prolonged exposure. Cell viability remained at 100 % after 3 days of treatment and was still ~79 % after 7 days, in contrast to both 2D cultures (~55 and ~13 %, respectively) and static 3D models (~72 and ~27 %, respectively) [29]. These results demonstrate increased drug resistance in 3D systems, particularly under perfusion, compared to 2D monolayer cultures where the cells are directly exposed to the drug. Also, these results, together with those obtained in the present work, highlight the time-dependent effect of drug exposure, where the delayed cytotoxic effect may be attributed to the time required for intracellular drug accumulation, as well as to limited drug penetration into spheroid structures [8]. In compact spheroid structures, localized regions with reduced drug transport efficiency may exist, and the outer cell layers may consume doxorubicin before it can reach all the cells, preventing the drug from being lethal to the entire cell population. In addition, cells located within the spheroid interior may exhibit reduced proliferative and metabolic activity, which could further decrease their sensitivity to doxorubicin [30].

To further understand the experimental results and provide a quantitative basis for analyzing drug response, we developed a mathematical model adapted from literature [22] to describe doxorubicin transport, intracellular accumulation, and changes in cell number during the 3-day treatment of individual and loosely aggregated cells in the recirculating perfusion bioreactor system. The model proposed by Eliaz and coworkers [22], grounded in their experimental findings, assumes that the cytotoxic effect of doxorubicin is governed by the intracellular drug amount rather than the extracellular concentration, with the viable cell number determined by the balance between the cell proliferation rate and the drug-induced cell death rate after a lag phase [22].

Our model adequately described the first day of treatment when the cell distribution is relatively homogeneous and spheroid-like structures are not yet developed. The model included the delayed cytotoxic effect as a fixed lag phase, as observed experimentally, followed by a balance between cell proliferation and death rates. This resulted in apparently similar predicted viable cell number as that in the initially seeded samples, which was consistent with experimentally assessed same metabolic activity in these two sample groups. Thus, the model grasped the effect of a short-term drug exposure of individual cells. Still, it should be noted that a delayed cytotoxic effect can be incorporated into the model using approaches other than a fixed lag phase. For example, a transit compartment model incorporates a series of intermediate steps that allow for a more realistic description of the delay between drug exposure and effect, which may provide greater flexibility for modelling long-term drug responses [31].

During the subsequent 2 days of treatment, intracellular doxorubicin accumulation continued to increase following the daily replacement of the medium and addition of a fresh doxorubicin dose. The number of viable cells progressively decreased, and although the model does not explicitly include a saturation effect or a predefined survival plateau, unlike Hill-type or peak concentration models [19], it captured the persistence of viable cells after 3 days of treatment. However, the model predicted a substantially stronger treatment effect than that indicated by the experimental MTT results, which may be explained by the fact that model does not capture emergence of additional drug resistance mechanisms, such as possible drug efflux, intracellular redistribution, saturation of drug uptake or other adaptive cellular responses, making it challenging to establish a quantitative relationship between drug exposure and cellular response [20,21]. As a result, intracellular drug accumulation continuously increases in all viable cells equally during repeated dosing, leading to an overestimation of drug induced cell death. Still, the applied model offers a possibility to directly incorporate biological constraints, such as a maximum drug capacity per cell or intrinsic resistance in certain cell populations, to more accurately reflect observed survival plateaus. At the same time, the experimentally observed formation of spheroid-like structures, in which cells were better protected from drug exposure, would require an additional model term to account for the dynamics of drug diffusion and accumulation within these aggregates. These improvements would allow a more realistic description of doxorubicin accumulation and cytotoxicity in long-term perfusion cultures and could improve the prediction of viable cell numbers after prolonged treatments.

5. CONCLUSION

The present work successfully utilized a previously developed 3D osteosarcoma cell culture model based on macroporous composite alginate scaffolds and biomimetic perfusion bioreactor for studies of anticancer drug effects. Specifically, it was shown that the 3D model can be used to simulate both a post-surgery situation with residual cancer cells and neoadjuvant chemotherapy in a simplified model of a solid tumour. Doxorubicin applied at a concentration of 1 μg cm^{-3} for 1 and 3 days was shown to induce a delayed cytotoxic effect on individual cells, while it had minor effects on cell-aggregates and spheroid-like structures. Only after the 3-day exposure, individual cells were rarely observed. The mathematical model, incorporating doxorubicin transport, intracellular accumulation, and cell proliferation and death within the perfused scaffolds, adequately described the limited response observed after 1 day of treatment but overestimated the effect of the 3-day treatment. This work represents one of the rare attempts to adapt and utilize a mathematical model for describing drug effects in a 3D cell culture. However, the model did not account for the formation of cell aggregates, which may have protected cells from the drug. Incorporating this aspect could be an important direction for future model development.

Overall, the 3D osteosarcoma cell culture model proved to be a robust platform for further studies of anticancer drug effects, while the developed mathematical model provides a foundation for future enhancements, including the incorporation of more complex cellular resistance mechanisms and terms describing drug diffusion and accumulation within spheroids.

SUPPLEMENTARY MATERIAL

Additional data are available electronically at https://www.ache-pub.org.rs/index.php/HemInd/article/view/1733, or from the corresponding author on request.

Acknowledgements: *This research was funded by the Science Fund of the Republic of Serbia (grant no.7503, "Bioengineered Tumor"). This work is also supported by the Ministry of Science, Technological Development and Innovation of the Republic of Serbia (Contract No. 451-03-34/2026-03/200135 and 451-03-34/2026-03/200110).*

REFERENCES

[1] Hosseini H, Heydari S, Hushmandi K, Daneshi S, Raesi R. Bone tumors: a systematic review of prevalence, risk determinants, and survival patterns. *BMC Cancer*. 2025; 25(1): 321. https://doi.org/10.1186/s12885-025-13720-0

[2] Cole S, Gianferante DM, Zhu B, Mirabello L. Osteosarcoma: A Surveillance, Epidemiology, and End Results program-based analysis from 1975 to 2017. *Cancer*. 2022; 128(11): 2107–18. https://doi.org/10.1002/cncr.34163

[3] Misaghi A, Goldin A, Awad M, Kulidjian AA. Osteosarcoma: a comprehensive review. *SICOT J*. 2018; 4: 12. https://doi.org/10.1051/sicotj/2017028

[4] Zhang Y, Yang J, Zhao N, Wang C, Kamar S, Zhou Y, He Z, Yang J, Sun B, Shi X, Han L, Yang Z. Progress in the chemotherapeutic treatment of osteosarcoma (Review). *Oncol Lett*. 2018. https://doi.org/10.3892/ol.2018.9434

[5] Lieu CH, Tan A-C, Leong S, Diamond JR, Eckhardt SG. From bench to bedside: lessons learned in translating preclinical studies in cancer drug development. *J Natl Cancer Inst*. 2013; 105(19): 1441-1456. https://doi.org/10.1093/jnci/djt209

[6] Pu F, Guo H, Shi D, Chen F, Peng Y, Huang X, Liu J, Zhang Z, Shao Z. The generation and use of animal models of osteosarcoma in cancer research. *Genes Dis*. 2024; 11(2): 664-674. https://doi.org/10.1016/j.gendis.2022.12.021

[7] Esposito A, Ferraresi A, Vallino L, Garavaglia B, Dhanasekaran DN, Isidoro C. Three-Dimensional *In Vitro* Cell Cultures as a Feasible and Promising Alternative to Two-Dimensional and Animal Models in Cancer Research. *Int J Biol Sci*. 2024; 20(13): 52935311. https://doi.org/10.7150/ijbs.96469

[8] Baek N, Seo OW, Kim M, Hulme J, An SSA. Monitoring the effects of doxorubicin on 3D-spheroid tumor cells in real-time. *Onco Targets Ther*. 2016; 9: 7207-7218. https://doi.org/10.2147/OTT.S112566

[9] Wan X, Li Z, Ye H, Cui Z. Three-dimensional perfused tumour spheroid model for anti-cancer drug screening. *Biotechnol Lett*. 2016; 38(8): 1389-1395. https://doi.org/10.1007/s10529-016-2035-1

[10] Banicevic I, Milosevic M, Petrovic J, Milivojevic M, Gasik M, Stojkovska J, Obradovic B. Macroporous alginate scaffolds with calcium phosphate filler as a 3D in vitro microenvironment supporting bone cancer cells. *International Journal of Polymeric Materials and Polymeric Biomaterials*. 2026; 75(7): 820-834. https://doi.org/10.1080/00914037.2025.2608101

[11] Lin H, Yeh Y. Porous alginate/hydroxyapatite composite scaffolds for bone tissue engineering: Preparation, characterization, and *in vitro* studies. *J Biomed Mater Res B Appl Biomater*. 2004; 71B(1): 52-65. https://doi.org/10.1002/jbm.b.30065

[12] Iglesias-Mejuto A, García-González CA. 3D-printed alginate-hydroxyapatite aerogel scaffolds for bone tissue engineering. *Materials Science and Engineering: C*. 2021; 131: 112525. https://doi.org/10.1016/j.msec.2021.112525

[13] Bose S, Roy M, Bandyopadhyay A. Recent advances in bone tissue engineering scaffolds. *Trends Biotechnol*. 2012; 30(10): 546-554. https://doi.org/10.1016/j.tibtech.2012.07.005

[14] Lee SS, Du X, Kim I, Ferguson SJ. Scaffolds for bone-tissue engineering. *Matter*. 2022; 5(9): 2722-2759. https://doi.org/10.1016/j.matt.2022.06.003

[15] Martin I, Wendt D, Heberer M. The role of bioreactors in tissue engineering. *Trends Biotechnol*. 2004; 22(2): 80-86. https://doi.org/10.1016/j.tibtech.2003.12.001

[16] Hirt C, Papadimitropoulos A, Muraro MG, Mele V, Panopoulos E, Cremonesi E, Ivanek R, Schultz-Thater E, Droeser RA, Mengus C, Heberer M, Oertli D, Iezzi G, Zajac P, Eppenberger-Castori S, Tornillo L, Terracciano L, Martin I, Spagnoli GC. Bioreactor-engineered cancer tissue-like structures mimic phenotypes, gene expression profiles and drug resistance patterns observed "in vivo". *Biomaterials*. 2015; 62: 138-146. https://doi.org/10.1016/j.biomaterials.2015.05.037

[17] Friedrich J, Seidel C, Ebner R, Kunz-Schughart LA. Spheroid-based drug screen: considerations and practical approach. *Nat Protoc*. 2009; 4(3): 309-324. https://doi.org/10.1038/nprot.2008.226

[18] Kim M, Gillies RJ, Rejniak KA. Current Advances in Mathematical Modeling of Anti-Cancer Drug Penetration into Tumor Tissues. *Front Oncol*. 2013; 3: 278. https://doi.org/10.3389/fonc.2013.00278

[19] El-Kareh AW, Secomb TW. Two-mechanism peak concentration model for cellular pharmacodynamics of Doxorubicin. *Neoplasia*. 2005; 7(7): 705-713. https://doi.org/10.1593/neo.05118

[20] Januškevičienė I, Petrikaitė V. Exploring doxorubicin transport in 2D and 3D models of MDA-MB-231 sublines: impact of hypoxia and cellular heterogeneity on doxorubicin accumulation in cells. *Am J Cancer Res*. 2024; 14(7): 3584-3599. https://doi.org/10.62347/VNWH9165

[21] Szakács G, Paterson JK, Ludwig JA, Booth-Genthe C, Gottesman MM. Targeting multidrug resistance in cancer. *Nat Rev Drug Discov*. 2006; 5(3): 219-234. https://doi.org/10.1038/nrd1984

[22] Eliaz RE, Nir S, Marty C, Szoka FC. Determination and modeling of kinetics of cancer cell killing by doxorubicin and doxorubicin encapsulated in targeted liposomes. *Cancer Res*. 2004; 64(2): 711-718. https://doi.org/10.1158/0008-5472.can-03-0654

[23] Stojkovska J, Zvicer J, Andrejevic M, Janackovic D, Obradovic B, Veljovic DN. Novel composite scaffolds based on alginate and Mg-doped calcium phosphate fillers: Enhanced hydroxyapatite formation under biomimetic conditions. *J Biomed Mater Res B Appl Biomater*. 2021; 109(12): 2079-2090. https://doi.org/10.1002/jbm.b.34856

[24] Stojkovska J, Zvicer J, Milivojevic M, Petrovic I, Stevanovic M, Obradovic B. Validation of a novel perfusion bioreactor system in cancer research. *Hem Ind*. 2020; 74(3): 187–96. https://doi.org/10.2298/HEMIND200329015S

[25] Gamble M. The Hematoxylins and Eosin. Theory and Practice of Histological Techniques. Elsevier; 2008;121-134. https://doi.org/10.1016/B978-0-443-10279-0.50016-6

[26] Kong Q, Siauw T, Bayen AM. *Python programming and numerical methods: a guide for engineers and scientists*. Academic Press; 2020. https://shop.elsevier.com/books/python-programming-and-numerical-methods/kong/978-0-12-819549-9

[27] Tu B, Zhu J, Liu S, Wang L, Fan Q, Hao Y, Fan C, Tang T-T. Mesenchymal stem cells promote osteosarcoma cell survival and drug resistance through activation of STAT3. *Oncotarget*. 2016; 7(30): 48296-48308. https://doi.org/10.18632/oncotarget.10219

[28] Yang J, Ma Z, Wang Y, Wang Z, Tian Y, Du Y, Bian W, Duan Y, Liu J. Necrosis of osteosarcoma cells induces the production and release of high-mobility group box 1 protein. *Exp Ther Med*. 2017; 15: 461-466. https://doi.org/10.3892/etm.2017.5415

[29] Abdollahzadeh H, Amoabediny G, Haghiralsadat F, Rahimi F, Adibfar A. Liposomal Doxorubicin Kinetic Study in an In vitro 2D and 3D Tumor Model for Osteosarcoma in a Perfusion Bioreactor. *Pharm Nanotechnol*. 2023; 11(5): 447-459. https://doi.org/10.2174/2211738511666230501202946

[30] Minchinton AI, Tannock IF. Drug penetration in solid tumours. *Nat Rev Cancer*. 2006; 6(8): 583-592. https://doi.org/10.1038/nrc1893

[31] Lobo ED, Balthasar JP. Pharmacodynamic modeling of chemotherapeutic effects: Application of a transit compartment model to characterize methotrexate effects *in vitro*. *AAPS PharmSci*. 2002; 4(4): 212-222. https://doi.org/10.1208/ps040442

Evaluacija 3D modela osteosarkoma: eksperimentalna studija i matematičko modelovanje odgovora na lek

Marija B. Pavlović[1], Ivana D. Banićević[1], Radmila M. Janković[2], Jasmina J. Stojkovska[1] and Bojana M. Obradović[1]

[1]Univerzitet u Beogradu, Tehnološko-metalurški fakultet, Beograd, Srbija
[2]Univerzitet u Beogradu, Medicinski fakultet, Beograd, Srbija

(Naučni rad)

Izvod

Osteosarkom i dalje predstavlja značajan klinički izazov, sa lošim ishodima u slučaju metastaza i sporim napretkom u razvoju novih terapija. U ovom radu je prethodno razvijen 3D model osteosarkoma, koji se sastoji od makroporoznih alginatnih nosača sa česticama hidroksiapatita, koji oponašaju koštano tkivo, i protočnog bioreaktora, procenjen kao alat za ispitivanje antitumorskih lekova. Ćelija mišjeg osteosarkoma (K7M2-wt) zasejane su na nosače (15×10^6 ćelija po cm^3) i gajene jedan dan u statičnim uslovima. U dve eksperimentalne serije nosači su potom izloženi doksorubicinu (1 μg cm^{-3}) u protočnim uslovima tokom 1 ili 3 dana (površinska brzina 40 μm s^{-1}), čime su simulirani uslovi nakon resekcije tumora, sa pretežno pojedinačnim ili slabo agregiranim ćelijama. U dve dodatne serije isti tretmani primenjeni su nakon 7 dana protočne kulture, kada su se formirali kompaktni sferoidi, čime je simuliran razvijen tumor. Histološka analiza i MTT test korišćeni su za procenu morfologije ćelija i njihove metaboličke aktivnosti. Kratkotrajni tretman imao je zanemarljiv efekat, dok je produžena izloženost značajno smanjila metaboličku aktivnost pojedinačnih ćelija, dok su sferoidne strukture pokazale povećanu otpornost na doksorubicin. Radi objašnjenja rezultata dobijenih u prve dve eksperimentalne serije, razvijen je matematički model koji opisuje transport leka, intracelularnu akumulaciju, proliferaciju ćelija i njihovo odumiranje. Model je uspešno opisao početnu fazu tretmana, ali je precenio efekat produžene izloženosti, ukazujući na mogućnost postojanja dodatnih mehanizama rezistencije. Sveukupno, rezultati potvrđuju potencijal ovog 3D modela za ispitivanje antitumorskih lekova.

Ključne reči: K7M2-wt ćelijska linija; protočni bioreaktor; alginatni nosač; doksorubicin; testiranje antitumorskih lekova; sferoidi

Preparation and characterization of activated carbon obtained from apricot pits for Cu(II) removal from aqueous solutions

Liliya Manoilova[1], Kamelia Ruskova[2], Metodi Mladenov[1], Vesislava Toteva[1] and Georgi Georgiev[1]

[1]*Faculty of Chemical Technology, University of Chemical Technology and Metallurgy, Sofia, Bulgaria*
[2]*Department of Chemistry, Faculty of Electronic Engineering and Technologies, Technical University of Sofia, Sofia, Bulgaria*

Abstract

Wastewater from chemical, petrochemical, and metallurgical industries contains different dissolved pollutants, characterized with high toxicity. In recent decades, industrial water treatment to remove heavy metal ions has become increasingly important due to their toxicity and the potential risk of accumulation in the food chain. This requires the application of various methods to reduce heavy metal ion concentrations to acceptable levels. In this respect, adsorption processes based on different sorbents are widely used for industrial wastewater treatment. For this investigation, apricot pits were pyrolyzed and chemically activated with potassium hydroxide to produce activated carbon. The adsorption capacity of the resulting material for removing Cu(II) ions from aqueous solutions was then investigated. The results have shown that these carbon-based adsorbents possess a high surface area and favourable textural characteristics, making them promising candidates for the removal of copper ions from aqueous solutions.

Keywords: Adsorption, active carbon, copper ions, water treatment, safety consumption.

Available on-line at the Journal web address: http://www.ache.org.rs/HI/

TECHNICAL PAPER

UDC 661.183.2:634.21:546.562

Hem. Ind. **80(2)** 87-94 (2026)

1. INTRODUCTION

Water is essential for life on Earth, and access to clean water is critical for both humans and ecosystems. Water quality depends on its physicochemical and biological parameters. Changes in parameters such as pH, temperature and heavy metal content in can render water unsafe for human consumption [1].

The problem of water contamination today is very relevant in connection with the prolonged increase of Anthropogenic pressure on the environment. High water pollution with toxic substances requires adoption of immediate measures to reduce the environmental risk, otherwise the water resources of the planet will be in a catastrophic state [2].

Organic matter, nutrients, pharmaceutical and personal care products, poly- and perfluoroalkyl substances, biocides, heavy metals, dyes, radionuclides, plastics, nanoparticles and pathogens are among the pollutants of major concern. Heavy metal ions are among the most spread contaminants. Heavy metals and metalloids are the elements with an atomic density greater than 4 g cm^{-3} including copper (Cu), cadmium (Cd), zinc (Zn), lead (Pb), mercury (Hg), arsenic (As), silver (Ag), chromium (Cr), iron (Fe) and platinum (Pt). These toxic metals are released daily into aqueous environment from diverse natural and anthropogenic sources. In many regions the average concentrations of Cr, Mn, Fe, Co, Ni, As and Cd found in surface water exceeds the permissible limits for drinking water [3-4].

Nowadays purification processes based on the adsorption methods are widely used for industrial wastewater treatment. Activated carbons are among the most versatile adsorbents, due to their properties that meet the increasing requirements for drinking water purity. Advances in modern technology have continually enhanced the quality and effectiveness of activated carbons [5].

One of the main methods for producing activated carbon involves the carbonization of carbon-containing materials, followed by chemical activation to increase the specific surface area and develop a porous texture. The main selection

Corresponding authors: Liliya Manoilova E-mail: lili_manoilova@abv.bg; https://orcid.org/0009-0002-8218-0393 Faculty of Chemical Technology, University of Chemical Technology and Metallurgy, Sofia, Bulgaria
Co-authors: Kamelia Ruskova https://orcid.org/0009-0006-7719-9419, Metodi Mladenov https://orcid.org/0000-0002-8548-1856, Vesislava Toteva https://orcid.org/0000-0002-5366-8798 and Georgi Georgiev https://orcid.org/0009-0005-9752-7654

Paper received: 9 January 2025; Paper accepted: 15 June 2026; Paper published: 20 June 2026.
https://doi.org/10.2298/HEMIND250109006M

criteria for activated carbon for specific applications include texture parameters (such as specific surface area, total pore volume, meso- and micropore volumes, and pores size distribution), the chemical nature of the surface (presence of functional oxygen groups), granulometric composition (dispersity), and mechanical properties, among others. It has been established that the high sorption capacity of activated carbons for metal ions in aqueous solutions is mainly due to the presence of oxygen-containing functional groups on their surface. The applications of activated carbons are largely determined by their specific surface area and the characteristics of their porous texture [6-7].

The aim of the present paper was to investigate the relationship between the porous texture and chemical nature of the surface of activated carbon obtained from apricot pits, and to evaluate the sorption capacity and their suitability for wastewater treatment, contaminated with Cu^{2+} ions.

2. EXPERIMENTAL

2. 1. Procedure of obtaining of activated carbon

Activated carbon (AC) was obtained from apricot pits, pyrolyzed at 700 ^{o}C for 1 h (Figure 1). Then the obtained material was milled and mixed homogeneously with activating agent KOH (Merck, *p.a., Germany*). Two samples with different mass ratios AC:KOH were investigated: 1 : 1 and 1 : 2 AC : KOH, labelled as ACCA1 and ACCA2. The chemical activation process with potassium hydroxide was carried out in a tube vacuum furnace at 500 °C for 1 hour. The samples obtained were neutralized with an appropriate amount of 10 wt.% HCl (Valerus, *p.a.*, Bulgaria) to remove the residual chemicals after the activation process. The obtained samples were washed multiple times with distilled water until neutrality. Finally, the AC samples were subjected to drying at 110 °C for 12 hours.

Figure 1. *Carbonized apricot pits and AC after carbonization*

2. 2. Experimental procedures

Elemental analysis was performed using a EuroEA Analyzer, model 3000 (manufacturer, country), to determine the elemental composition and weight, wt.% of carbon, hydrogen and nitrogen in the activated carbon samples. The oxygen content was calculated by difference, based on these measurements.

The porous texture of the obtained AC samples was characterized by measuring nitrogen ~~№~~ adsorption isotherms at 77 K on an automatic gas adsorption porosimeter Surfer (Thermo Scientific, United States). The specific surface area was determined using Brunauer-Emmett-Teller (BET) method [8]. The total pore volume (V_t) was determined at a relative pressure P_i/P_0 = 0.9, where P_i is the real gas pressure during the measurement, and P_0 is the saturated vapor pressure of the same gas at the temperature of the experiment measurement.

Surface chemistry of the AC samples was analysed by a Fourier transform infrared (FTIR) spectrometer (Nicolet Avatar 360 FTIR spectrometer, Germany) and registered in the region 500 to 4000 cm^{-1}. The spectra were recorded at a spectral resolution of 2 cm^{-1} and accumulation of 64 scans.

The iodine number of AC samples was determined by a standard test method [9] presenting the amount of iodine absorbed (in mg) by 1 g of the material.

The surface morphology of activated carbons was analysed using scanning electron microscopy coupled with energy-dispersive X-ray spectroscopy (SEM-EDX) by a JEOL JSM-6390 instrument (Philips, Germany). The measurement was done with high resolution in mode 10 kV, 0° and 0.1 mm scan spacing.

2. 3. Procedure for adsorption capacity measurement

The adsorption capacity of the activated carbons in regard to Cu^{2+} ions was determined using the following methodology: aqueous solution of $CuSO_4.5H_2O$ (Valerus, *p.a.*, *Bulgaria*) at the concentration of 5 g L^{-1} was prepared. Precisely determined amounts of the $CuSO_4 \times 5H_2O$ solution (10, 20, 30, 40 and 50 mL) were taken and transferred into ~~to~~ flasks. Then samples, labelled as K1 to K4 were diluted with distilled water to 50 mL to obtain the corresponding concentrations K1 to K5. The adsorption experiments were conducted using 0.2 g of activated carbon (type ACCA2) for each flask followed by homogenization for 1 h at 25 ± 2 °C. The initial pH of the copper solutions was in the range pH 4.0 to 4.5, while after the adsorption the final pH value was in the range 6.0 to 6.5. The initial and residual concentrations of Cu^{2+} ions in the solutions were determined with UV-VIS Spectrophotometer, by using the cuprizone [10]. After the treatment with AC, the concentration of Cu(II) ions decreased, and nearly complete removal of the metal ions was recorded. As a result, the pH values change from acidic to approximately neutral. All adsorption experiments were performed in five replicates, and reported values correspond to the average values obtained.

3. RESULTS AND DISCUSSION

3. 1. Elemental composition analysis

The results of the elemental analysis of the AC samples are presented in Table 1.

Table 1. *Elemental composition of the activated carbon samples*

Sample	Content, wt.%			
	Carbon	Hydrogen	Nitrogen	Oxygen
ACCA1	95.29	2.69	< 0.01	2.02
ACCA2	77.34	3.33	< 0.01	19.33

The elemental composition of the obtained activated carbon is characterized by high carbon contents (~77 to 95 wt.%) and low hydrogen contents (up to 3.33 wt.%) for both ACCA1 and ACCA2 samples. There was an increase in the oxygen content in the sample activated with a higher ratio AC:KOH. In specific, the oxygen content increased from ~2 wt.% in ACCA1 to ~19 wt.% in ACCA2 because of the activation process, confirmed by FTIR spectra, showing the formation of significant amounts of oxygen-containing forms on the carbon surface.

3. 2. Adsorption-textural parameters determined by BET analysis

The results of the textural analysis of the AC samples are shown in Table 2.

Table 2. *Specific surface area and basic textural parameters of the activated carbons*

Sample	S_{BET} / m^2g^{-1}	V_{micro} / cm^3g^{-1}	V_{mezo} / cm^3g^{-1}	V_{micro} / %	V_{mezo} / %	V_t / cm^3g^{-1}
ACCA1	929	0.3626	0.1213	74.9	25.1	0.4839
ACCA2	1003	0.3882	0.1459	72.7	27.3	0.5341

The data in Table 2 show that ACCA2 is characterized by a high specific surface area (S_{BET} = 1003 m^2 g^{-1}) and total pore volume (V_t = 0.5341 cm^3 g^{-1}) compared with the results determined for the sample ACCA1 (S_{BET} = 929 m^2 g^{-1} and V_t = 0.4839 cm^3 g^{-1}). The nitrogen adsorption-desorption isotherms of activated carbon samples ACCA1 and ACCA2 are presented in Figures 2 and 3.

According to the IUPAC classification, the nitrogen adsorption isotherms of the samples correspond to Type I, which is typical of micro-mesoporous textures. The part of the isotherms of relatively low pressures (relative pressure around 0.05 to

0.1) corresponds to micropores filling with tendency to saturation near 0.3 typical for microporous adsorbents. A higher saturation pressure in the sample ACCA2 shows a more developed porous texture of the obtained activated carbon.

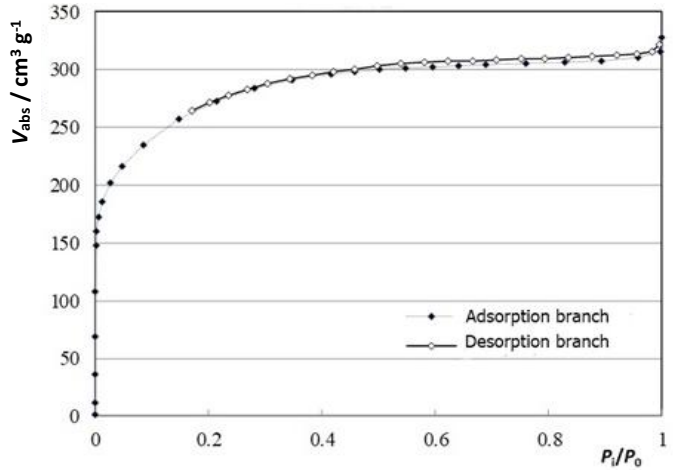

Figure 2. *Low-temperature nitrogen adsorption-desorption isotherm for the ACCA1 sample*

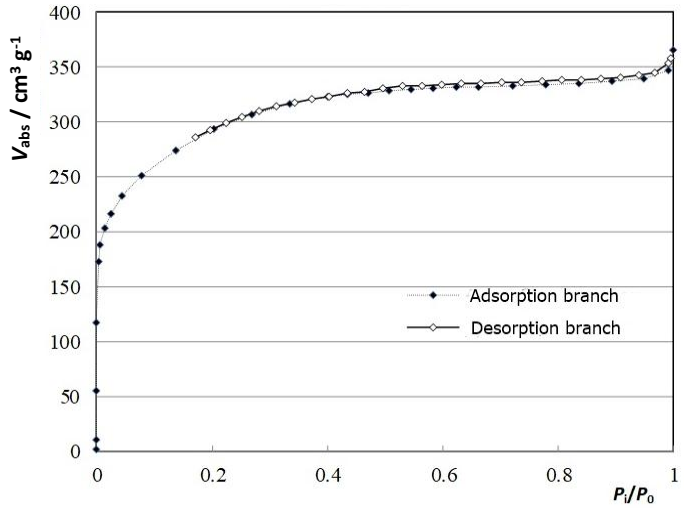

Figure 3. *Low-temperature nitrogen adsorption-desorption isotherm for the ACCA2 sample*

3. 3. Fourier transform infrared spectroscopy analysis

The FTIR spectra of the obtained adsorbents ACCA1 and ACCA2 are presented in Figure 4.

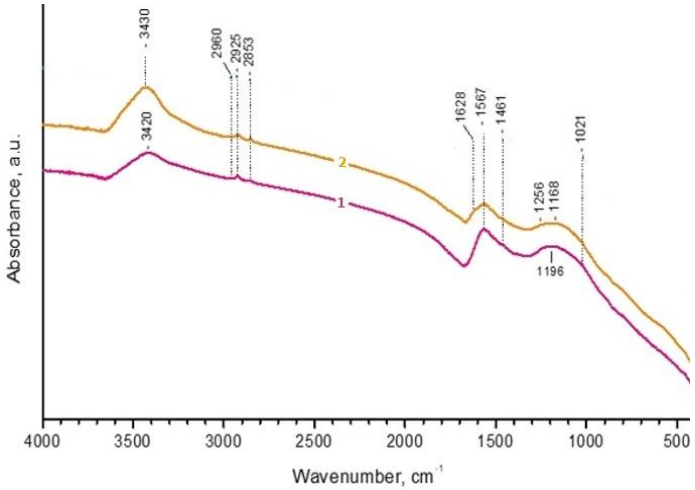

Figure 4. *Fourier transform infrared spectra of 1 - ACCA1 and 2 - ACCA2 samples*

The absorption peak at 3430 cm^{-1} can be attributed to the stretching vibration of -OH groups, which is characteristic of hydroxyl functional groups and typically appears in the 3500 to 3700 cm^{-1} range. The bands around 2900 cm^{-1} are due to aliphatic C-H structures. The peaks about 1570 and 1630 cm^{-1} are due to stretching vibration of the C=C functional group [11].

The absorption bands in the 1260 to 1050 cm^{-1} region are attributed to C–O stretching vibrations of oxygen-containing functional groups present on the carbon surface. The bands around 1400 cm^{-1} may be associated with O–H bending vibrations, C–H deformation, or symmetric stretching of carboxylate groups [12].

3. 4. Iodine number

The iodine number is a measure of the relative activation level of carbons by adsorption of iodine from an aqueous solution, where a higher value indicates a higher degree of activation. The Iodine number determined for the sample ACCA1 was 599.8 mg g^{-1} versus 710.1 mg g^{-1} determined for the ACCA2 sample. This indicates that the sample with higher content of activating agent should have better adsorption properties. This agrees with the increased surface area for the sample activated with the higher content of activating agent, confirmed by the BET analyses.

3. 5. Scanning electron microscopy

The surface morphology of activated carbons was analysed using SEM-EDX technique showing similar features. Figure 5 shows micrographs of the ACCA2 sample, which was selected for its well-developed micro- and mesoporous structure and higher specific surface area, resulting from chemical activation with KOH, as confirmed by BET analysis.

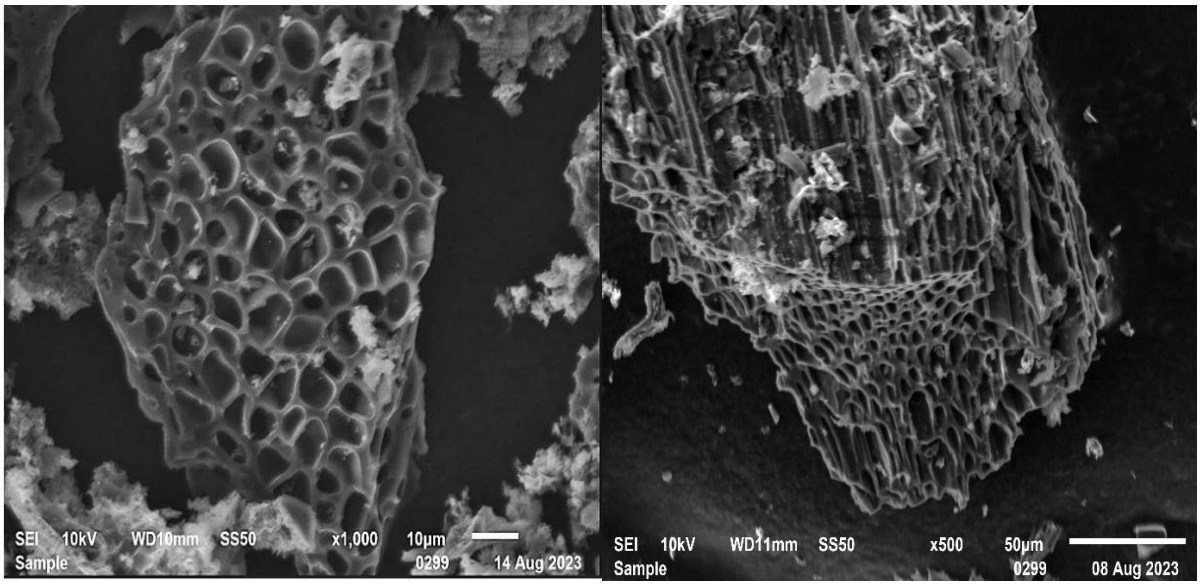

Figure 5*. SEM images of the ACCA2 sample at different magnifications*

3. 6. Adsorption capacity of the activated carbons for Cu(II) ions in aqueous solutions

The amount of Cu(II) ions adsorbed by ACCA2 was determined by calculating the difference between the initial ion concentration and the concentration measured after the homogenization. The measured concentrations in the initially prepared solutions and after the adsorption experiments are shown in Table 3.

Table 3*. Measured Cu(II) concentrations by UV-VIS analysis before and after the adsorption experiments using ACCA2*

Solution	Initial concentration of Cu^{2+}, g L^{-1}	Residual concentration of Cu^{2+}, g L^{-1}
K1	0.933	0.737
K2	1.867	1.424
K3	2.800	1.915
K4	3.734	2.996
K5	4.667	4.371

The UV-VIS analysis confirmed that the activated carbon type ACCA2 produced from apricot pits generally reduces the concentration of copper ions in the investigated solutions. The highest adsorbed amounts were observed in solutions K3 and K4, in which the Cu(II) concentrations decreased to ~1.9 and 3.0 g L^{-1}, respectively. The highest adsorption capacity was observed for sample K3 where the adsorbed amount of copper per mass of the adsorbent was 221.2 mg g^{-1}. Further increases in the initial Cu(II) concentration did not lead to the increase in adsorption capacity, indicating possible saturation of active adsorption sites.

4. CONCLUSIONS

The results obtained show that produced activated carbons ACCA1 and ACCA2 are with high specific surface area and well developed micro- and mesopores structure. The sample ACCA2 activated with a higher content of the activating agent has shown better texture parameters. In addition, chemical activation with potassium hydroxide increases the number of hydroxyl groups, which in turn favours metal ion adsorption. Cu(II) ion adsorption studies confirmed that the activated carbon produced from apricot pits generally reduces the ion concentration in the investigated solutions. All those results permit us to conclude that the generated ACs can be used effectively as adsorbents in liquid-phase applications and water purification processes.

Acknowledgement: *The study is funded by the European Union-Next GenerationEU, through the National Recovery and Resilience Plan of the Republic of Bulgaria, project № BG-RRP-2.004-0002, „BiOrgaMCT".*

REFERENCES

[1] Zhang P, Yang M, Lan J, Huang Y, Zhang J, Huang S, Yang Y, Ru J. Water Quality Degradation Due to Heavy Metal Contamination: Health Impacts and Eco-Friendly Approaches for Heavy Metal Remediation, *Toxics*. 2023; 11: 828. https://doi.org/10.3390/toxics11100828

[2] Trus I, Gomelya M, Vorobyova V, Skiba M. Effectiveness of complexation-nanofiltration during water purification from copper ions, *J Chem Techno. Metall.* 2021; 56 (5): 1008-1015. https://journal.uctm.edu/node/j2021-5/16_20-65_p_1008-1015.pdf

[3] Zamora-Ledezma C, Negrete-Bolagay D, Figueroa F, Zamora-Ledezma E, Ni M, Alexis F, Guerrero V. Heavy metal water pollution: A fresh look about hazards, novel and conventional remediation methods, *Environ Technol Innov.* 2021; 22: 101504. https://doi.org/10.1016/j.eti.2021.101504.

[4] Koliehova A, Trokhymenko G, Magas N, Gomelya N, Trus I. Study of the Process of Electro Evolution of Copper Ions from Waste Regeneration Solutions, *J Ecol Eng.* 2020; 21(2): 29-38. https://doi.org/10.12911/22998993/116351.

[5] Monser L, Adhoum N., Modified activated carbon for the removal of copper, zinc, chromium and cyanide from wastewater, *Separ Purif Technol.* 2002; 26: 137-146. https://doi.org/10.1016/S1383-5866

[6] Boehm H. Some aspects of the surface chemistry of carbon blacks and other carbons, *Carbon* 1994; 32(5): 759-769. https://doi.org/10.1016/0008-6223(94)90031-0

[7] Bhatnagar A, Hogland W, Marques M, Sillanpaa M. An overview of the modification methods of activated carbon for its water treatment applications, *Chem Eng J.* 2013; 499-511. https://doi.org/10.1016/j.cej.2012.12.038

[8] Determination of the specific surface area of solids by gas adsorption-BET method, *ISO 9277:2022*, 2022. https://www.iso.org/standard/44941.html

[9] Freese SF, Trollip DL, Nozaic DJ. Manual for testing of water and wastewater treatment chemicals, WRC Report No: 1184/1/04. ISBN No: 1-77005-101-5, 2004. https://www.wrc.org.za/wp-content/uploads/mdocs/1184-1-041.pdf

[10] Bulgarian Institute for Standardization, БДС 6401:1979. Reagents. Determination of copper impurity content by colorimetric methods. https://bds-bg.org/bg/project/show/bds:proj:25205 (in Bulgarian)

[11] Gomez-Serrano I, Piriz-Almeida F, Duran-Valle C, Pastor Villegas J. Formation of oxygen structures by air activation, A study by FT-IR spectroscopy, *Carbon.* 1999; 37: 1517-1528. https://doi.org/10.1016/S0008-6223(99)00025-1

[12] Hendawy A. Variation in the FTIR spectra of a biomass under impregnation, carbonization and oxidation conditions, *J Anal Appl Pyrol.* 2006: 75: 159. https://doi.org/10.1016/j.jaap.2005.05.004.

Priprema i karakterizacija aktivnog uglja iz koštica kajsije za uklanjanje Cu(II) jona iz vodenih rastvora

Liliya Manoilova[1], Kamelia Ruskova[2], Metodi Mladenov[1], Vesislava Toteva[1] i Georgi Georgiev[1]

[1]*Faculty of Chemical Technology, University of Chemical Technology and Metallurgy, Sofia, Bulgaria*
[2]*Department of Chemistry, Faculty of Electronic Engineering and Technologies, Technical University of Sofia, Sofia, Bulgaria*

(Stručni rad)

Izvod

Otpadne vode iz hemijske, petrohemijske i metalurške industrije sadrže različite rastvorene zagađujuće materije koje se odlikuju visokom toksičnošću. Tokom poslednjih decenija, tretman industrijskih otpadnih voda u cilju uklanjanja jona teških metala postao je od izuzetnog značaja zbog njihove toksičnosti i mogućnosti akumulacije u lancu ishrane. To zahteva primenu različitih metoda za smanjenje koncentracije jona teških metala na prihvatljiv nivo. U tom kontekstu, adsorpcioni procesi zasnovani na primeni različitih sorbenata široko se koriste za prečišćavanje industrijskih otpadnih voda. U ovom istraživanju, koštice kajsije su podvrgnute pirolizi i hemijskoj aktivaciji kalijum-hidroksidom radi dobijanja aktivnog uglja. Nakon toga ispitivan je adsorpcioni kapacitet dobijenog materijala za uklanjanje Cu(II) jona iz vodenih rastvora. Rezultati su pokazali da ovi adsorbenti na bazi ugljenika poseduju veliku specifičnu površinu i povoljne teksturalne karakteristike, što ih čini perspektivnim kandidatima za uklanjanje jona bakra iz vodenih rastvora.

Ključne reči: Adsorpcija, aktivni ugljenik, joni bakra, obrada otpadne vode, bezbedna potrošnja

Extraction of aliphatic hydrocarbons and formation of new ones at superheated steam temperatures from demineralized anthracite from Vrška Čuka (Serbia)

Amer M. Juma[1], Ljubiša B. Nikolić[1], Bratislav Ž. Todorović[1], Jelena S. Stanojević[1], Snežana S. Trifunović[2], Tanja Petrović Pantić[3] and Sanja M. Petrović[1]

[1]*University of Niš, Faculty of Technology, Leskovac, Serbia*
[2]*University of Belgrade, Faculty of Chemistry, Belgrade, Serbia*
[3]*Geological Survey Institute of Serbia, Belgrade, Serbia*

Abstract

Extraction of aliphatic hydrocarbons from demineralized coal using superheated steam is a promising method for reducing the industrial production costs. In the present study, extractions were performed at superheated steam temperatures without a catalyst (373 to 473 K; 2-20 h). The greatest yield of extracted organic matter was obtained during the first 2 h (4.0 to 6.1 % of the initial sample mass). At longer times, solubility values varied, suggesting that the release of aliphatic hydrocarbons depends on their location within different structural domains of the organic matrix. The high maturity of the organic matter indicates that the anthracite sample is in the metagenesis phase. Gas chromatography with flame ionization detection showed that extraction yielded n-paraffins, primarily the energetically significant C12 to C19 homologues, comprising 50 to 61 % of extracted compounds after 20 h. Comparison with less mature coals (lignite and brown coal) from the same area revealed a similar trend, though, with increasing coalification, the proportion of n-paraffins decreased and terpenes increased. Fourier transform infrared spectroscopy of the dry residue after extraction showed that methyl groups (2972 cm^{-1}) were lost after 2 hours at all temperatures, while complete removal of aliphatic structures, including ethyl groups (2924, 2852 and 1377 cm^{-1}), occurred after 20 h. The detected paraffins and terpenes originated from methyl and ethyl groups extracted from the organic matrix. Additionally, while lignite and brown coal gave nearly identical results, lignite lacked independently bound methyl groups.

Keywords: coal, solubility, maturation, paraffins, methyl groups.

Available on-line at the Journal web address: http://www.ache.org.rs/HI/

ORIGINAL SCIENTIFIC PAPER

UDC 661.716:553.93(497.11)

Hem. Ind. **80(2)** 95-106 (2026)

1. INTRODUCTION

The Triassic period brought significant changes to the planet's flora and fauna. For unknown reasons, at the end of this period (around 205 million years ago), a major biological crisis occurred, resulting in mass extinction (>70 %) of plant and animal species [1]. Geological records of this crisis on the Balkan peninsula are primarily found in Eastern Serbia (Carpatho-Balkan region). The extinction of flora led to the accumulation of dead plant material along the shores of the Carpathian Sea, as fluctuations in sea level (first retreating and then advancing) resulted in repeated deposition and coverage of organic matter in this area [2-5]. From the deposited material, anthracite deposits were formed in Vrška Čuka, Dobra and Jerma.

The Vrška Čuka mine is in eastern Serbia (the northernmost part of the Stara Planina mountain). The geology of this area, as well as the full succession of Jurassic rock layers, has been well studied [6-9]. The coal itself is of a black-grey colour, has a metallic-glass sheen, and, depending on its metamorphic state, can appear in graphite form. In recent years, there has been increasing discussion about the economic feasibility of exploiting this mine and the possibility of

Corresponding authors: Ljubiša Nikolić E-mail: nljubisa@yahoo.com; https://orcid.org/0000-0003-2886-6618 Faculty of Technology, Bulevar Oslobođenja 124, 16 000 Leskovac, Serbia
Co-authors: Amer M. Juma hhttps://orcid.org/0009-0003-0883-8297, Bratislav Ž. Todorović https://orcid.org/0000-0002-0820-4513, Jelena S. Stanojević https://orcid.org/0000-0001-7923-0770; Snežana S. Trifunović https://orcid.org/0000-0001-9528-6686; Tanja Petrović Pantić https://orcid.org/0000-0003-1456-6913 and Sanja M. Petrović https://orcid.org/0000-0001-9493-8355

Paper received: 16 July 2025; Paper accepted: 8 July 2026; Paper published: 31 July 2026.
https://doi.org/10.2298/HEMIND250719007J

its closure. Certainly, the economic development of this region is partially tied to this mine. The main issue is that this type of coal is not widely used but is rather employed for specific industrial needs. In this regard, it is necessary to find a new role for it in potential industrial production. This work provides a partial contribution to that effort.

The removal of aliphatic hydrocarbons from aromatic ones in geochemical studies using water extraction under supercritical conditions is relatively well-known (many authors). To date, this technique has primarily been used for the determination of aliphatic hydrocarbons in petroleum source rocks [10]. Besides water vapor, carbon dioxide with or without additives is also frequently used [11-12]. Additionally, there are reverse cases of extracting aromatic hydrocarbons from aliphatic chains [13]. Both extraction processes are part of modern industrial needs, particularly in the industries of plastics, rubber, adhesives, etc. Beyond the classic separation of aliphatic from aromatic compounds for industrial purposes, their separation can also be utilized for environmental purposes, where these compounds are present as pollutants in various types of soil [14]. Previous studies on anthracite from Vrška Čuka have shown a high presence of aromatic hydrocarbons [15,16] that are associated with aliphatic hydrocarbons in short chains. In the development and practical application of this technique, industrially and economically developed countries have played a significant role, particularly in advancing the technology of coal-to-liquid (CTL) conversion. The profitability of synthesizing new hydrocarbons from coal depends on the type of coal (its maturation), the quantity and quality of the fuel produced, as well as the environmental consequences of the technological process itself. The primary focus has been taken on using low-quality coal with a lower degree of maturation. In contrast, data published on the kinetics of CTL formation from anthracite, as well as its synthesis at lower temperatures without the use of catalysts, remain very scarce. Accordingly, this analysis focuses on the extraction of aliphatic hydrocarbon chains at superheated water vapor (SHWV) temperatures of 373-473 K.

There are several methods for extracting aliphatic compounds. The development of methods for recovering these compounds from natural resources such as oil and coal is of growing interest due to their increasing industrial applications [17]. Inexpensive methods are particularly important, as they reduce the costs of industrial production [18]. This focus on innovative extraction approaches has become especially relevant considering the continuously rising costs of industrial manufacturing [19]. Accordingly, in the present study, emphasis was placed on the recovery of aliphatic hydrocarbons from high calorific hard coals, such as anthracite, at different temperatures using SHWV.

2. EXPERIMENTAL

2. 1. Thermal solubility experiments

Coal samples of anthracite, brown coal and lignite were obtained from the surface coal dump. The samples were ground in a vibratory mill with a ceramic ball, at a vibration intensity of 8 on the instrument scale 018, for 30 min (VEB MLW Medizintechnik Leipzig, German Democratic Republic, GDR). Subsequently, the samples were dried for 12 h in a laboratory oven at 355 K and transferred to a desiccator, where they were kept until a constant mass was achieved. The procedure for separating inorganic fractions from kerogen in geological samples is well-established [20-22]. Coal samples were demineralized for 72 h using an HF (22 M)-HCl (12 M) mixture at 353 K, followed by treatment with boiling HCl (12 M) for 12 h. The obtained organic residue was thoroughly rinsed with deionized water (Fisher, HPLC grade; <0.1 μS), ensuring that that all residual acid was removed. Removal of bitumen was performed in a Soxhlet apparatus for 72 h at 355 K using a benzene/methanol azeotropic mixture (6:1, v/v; J.T. Baker, HPLC grade), until the solvent in the extraction flask became clear. After that, the demineralized coal sample was dried again to remove residual solvent (355 K, 8 h).

Each of the five demineralized coal samples (2.9990, 3.0015, 3.0020, 2.9900 and 3.0005 g) was accurately weighed and combined with 15 cm^3 of deionized water in a Teflon capsule (total volume 42.4 cm^3; free volume 24.4 cm^3). The capsules were sealed with Teflon lids and then placed into steel reactors (Figure 1), which ensured hermetic sealing. The lids and capsules were secured with steel screws. The reactors were placed in a muffle furnace and heated to 373, 398, 423, 448 and 473 K (Figure 2). The corresponding saturated pressure values of water at each temperature were taken from thermodynamic tables based on the liquid-vapor phase equilibrium as follows: 373 K - 100 kPa, 398 K - 230 kPa, 423 K - 480 kPa,

448 K - 890·kPa and 473 K - 1550·kPa. These values are determined solely by temperature and represent the equilibrium vapor pressure; they do not depend on the free volume in the reactor.

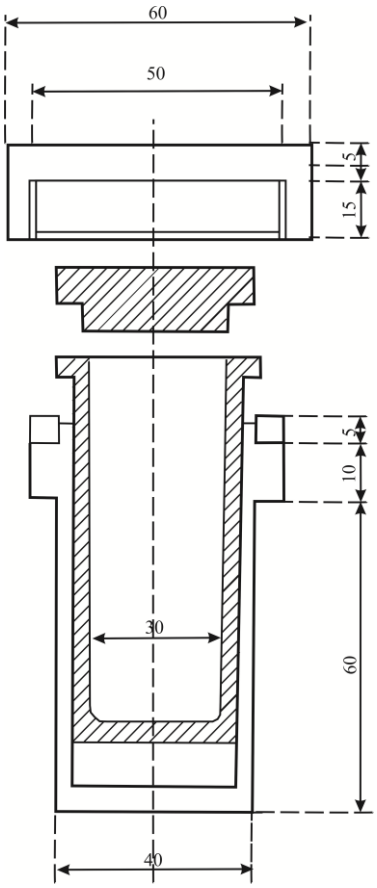

Figure 1. *Schematic representation of the reactor*

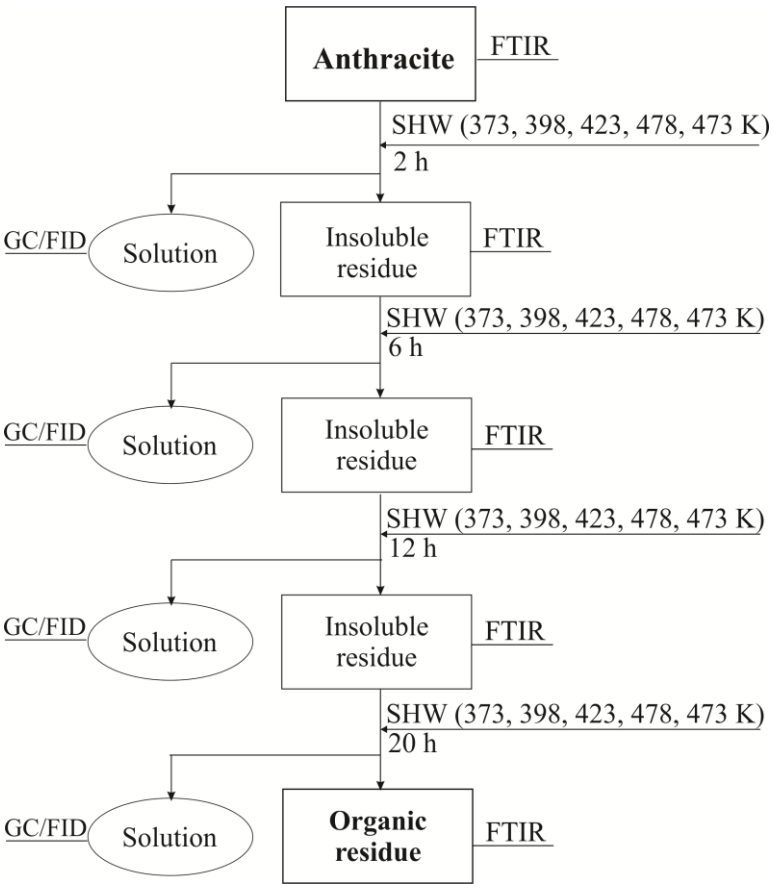

Figure 2. *Flow chart of extraction procedure*

After each extraction phase, the samples were filtered, dried, and the residue mass was measured. Portions of the solution and coal residue were preserved for chromatographic analysis and Fourier transform infrared (FTIR) spectroscopy, respectively. For each extraction, the mass of solution and coal residue recovered was calculated as a fraction of the initial sample mass. This procedure was repeated by heating the extraction residues for additional periods of 4, 6 and 8 hours after the initial 2-hour heating; at the start of each extraction, a fresh equal amount of deionized water was added. The total mass fraction recovered was obtained by summing the individual fractions from each extraction step.

The heating was conducted in a muffle furnace (Carbolite, Germany), with the temperature determined with an accuracy of ±2 K. This method is similar to the process of semicoke obtaining at low temperatures, with the research emphasis placed on the content and composition of the soluble phase. The research was carried out with 3 samples with 20 experiments each (5 different temperatures in four different intervals).

2. 2. Analytical methods

2. 2. 1. Ultimate analysis

Ultimate analysis was performed using a Vario EL III C, H, N, S/O Elemental Analyzer (ElementarAnalysensysteme GmbH, Hanau-Germany). This analysis was performed at the Faculty of Chemistry (University of Belgrade, Serbia) under the following conditions: the combustion temperature of 1150 °C, helium as the carrier gas and a thermal conductivity detector (TCD). The dynamic working range of the apparatus is as follows: C: 0.03 to 20.00 mg; H: 0.03 to 3.00 mg; N: 0.03 to 2.00 mg; S: 0.03 to 6.00 mg.

2. 2. 2. Gas chromatography-mass spectrometry and gas chromatography-flame ionization detection analysis

The same volume of each sample (1 cm^3) was transferred into test tubes, mixed with 1 cm^3 of *n*-hexane (LC-MS grade, Fisher Scientific, Germany) and vigorously shaken for 5 minutes. After shaking, the samples were allowed to stand for approximately 1 minute until clear phase separation occurred. The upper hexane layer was transferred by glass Pasteur pipettes directly into syringes fitted with 33 mm diameter PTFE sterile syringe filters (hexane-compatible, 0.45 µm pore size). A single extraction step by n-hexane was used. Filtered hexane extracts were subjected to GC/MS analysis performed using an Agilent Technologies 7890B gas chromatograph, equipped with a weakly polar silica capillary column, HP-5MS (5 % diphenyl- and 95 % dimethyl-polysiloxane, 30 m × 0.25 mm, 0.25 µm film thickness; Agilent Technologies, St. Louis, MO, USA), and coupled with an inert, selective 5977A mass detector of the same company. The samples (5 µl) were injected in spitless mode. Helium was used as the carrier gas at a constant flow rate of 1 ml min^{-1}. The oven temperature was programmed to rise from 353 to 583 K at a rate of 10 K min^{-1} and then held at 583 K for 10 min. The temperatures of the MSD transfer line, ion source, and quadruple mass analyser were set at 573, 500 and 423 K, respectively. The ionization voltage was 70 eV and the mass range *m*/*z* 35 to 650. The flows of the carrier gas (He), make up gas (N_2), fuel gas (H_2) and oxidizing gas (air) were 1, 25, 30 and 400 ml min^{-1}, respectively. The gas chromatography-mass spectrometry (GC/MS) and gas chromatography with flame ionization detection (GC/FID) analyses were performed at the Faculty of Technology, University of Niš, Serbia.

GC/FID analysis was carried out under identical experimental conditions as GC/MS. The temperature of the flame-ionization detector (FID) was set at 573 K. Data processing was performed using MSD Chem-Station (version F.01.00.1903), MassHunter Qualitative Analysis (version B.06.00) and AMDIS (version 2.70) software [23] (Agilent Technologies, USA). Baseline correction was carried out automatically by the software, while peak deconvolution and identification were performed using AMDIS with default settings. Manual reintegration was applied only when required in cases of overlapping peaks to ensure accurate peak area determination. Identification of extract constituents was based on comparison of the compounds' retention indices with those reported in the literature and comparison of their mass spectra with reference spectra from the Wiley 6 [24], NIST2011 [25] and RTLPEST3 [26] libraries. Retention indices of the components from the analysed samples were experimentally determined using a homologous series of *n*-alkanes from C_8-C_{20} and C_{21}-C_{40} as standards. The semi-quantitative composition (content, %) of the samples was determined by the area normalization method, based on the automatically integrated peak areas of the GC/FID signal, without any corrections.

2. 2. 3. Fourier transform infrared spectroscopy

Fourier transform infrared (FTIR) spectroscopy analysis was performed on the initial samples and on the dry residues after individual extraction stages. Anthracite, demineralized coal and demineralized coal residue were finely powdered and dispersed evenly in anhydrous potassium bromide (KBr) pellets (1 mg *per* 150 mg KBr). The mixture was then subjected to vacuuming and pressing under a pressure of 200 MPa to obtain the appropriate lozenges. FTIR spectra were obtained using a Bomem MB-100 spectrometer (Hartmann and Braun, Canada) set to generate uniform spectra (Faculty of Technology, University of Niš, Serbia). The acquisition parameters were as follows: spectral range 4000 to 400 cm^{-1}, 10 scans, and baseline treatment using interactive polynomial ($\underline{C}X^2$ and $\underline{D}X^3$). Background scanning was performed with a pellet made of anhydrous KBr.

3. RESULTS AND DISCUSSION

3. 1. Elemental analysis

Based on elemental analysis, the H/C and O/C ratios were calculated for all three coal samples analyzed (*i.e.* anthracite, brown coal, and lignite) and plotted on a van-Krevelen diagram. This diagram illustrates the maturation pathway of organic matter, distinguishing the diagenesis, catagenesis and metagenesis regions (Figure 3). Unlike anthracite from Vrška Čuka (metagenesis), brown coal from Sokobanja and lignite from Kostolac are characterized by a low degree of coalification and are still in the diagenesis stage. Based on these results and previous observations, it can be concluded that with increasing coalification, the proportion of n-paraffins decreases, while the proportion of terpenes increases.

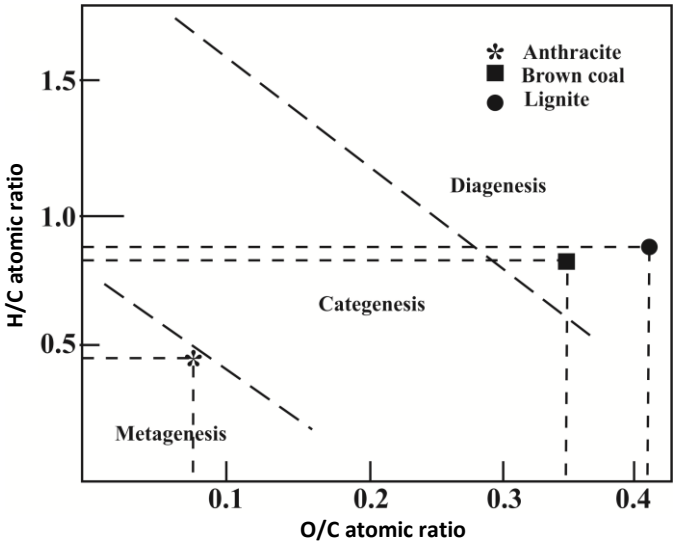

***Figure 3**. Van-Krevelen diagram for Vrška Čuka (anthracite), Sokobanja (brown coal) and Kostolac (lignite) coals*

3. 2. Thermal solubility experiments

As pointed out in the Experimental section, thermal solubility analyses of Vrška Čuka demineralized anthracite were performed at 373, 398, 423, 448 and 473 K (Table 1). At all temperatures, the greatest extraction of organic matter occurred within the first 2 h. After that, the extraction rate decreased over time, except in the case of the sample at 473 K, where solubility after 12 h was greater than after 6 h. This result may be due to further decomposition or transformation of organic molecules at higher temperatures, leading to the formation of additional soluble groups. This assumption is supported by the fact that after 12 h of extraction, there was no further decrease in the residue mass. Therefore, in addition to the diminishing amount of material available for extraction, the results of the thermal dissolution experiments do not show a linear trend, likely due to the dissolution and release of structurally diverse aliphatic chains at different temperatures and time intervals.

***Table 1**. Thermal solubility experiments of the Vrška Čuka demineralized anthracite*

Time, h	Content of dissolved organic matter (relative to initial demineralized sample mass) ± standard deviation, %				
	373 K	398 K	423 K	448 K	473 K
2	6.1±0.2	4.0±0.2	4.7±0.2	5.5±0.3	5.0±0.3
6	5.5±0.2	3.8±0.2	1.5±0.1	1.1±0.1	1.0±0.1
12	3.0±0.1	0.0±0.0	1.0±0.1	1.1±0.1	2.2±0.1
20	0.0±0.0	0.0±0.0	0.0±0.0	0.0±0.0	0.0±0.0
Total	14.6±0.5	7.8±0.4	6.3±0.4	7.7±0.5	8.2±0.5

The extraction results of this demineralized coal were compared with the extraction results of neighbouring coals of other types under the same conditions (Kostolac lignite and Sokobanja brown coal). The comparison results are presented in Table 2, showing that coal at a lower maturation stage exhibits better solubility.

***Table 2**. Comparison of thermal solubility results of the investigated demineralized coals after 2 h at different temperatures*

Sample	Contentof dissolved organic matter (relative to initial demineralized sample mass)) ± standard deviation, %				
	373 K	398 K	423 K	448 K	473 K
VČ	6.1±0.2	4.0±0.2	4.7±0.2	5.5±0.3	5.0±0.3
KL	15.3±0.7	13.2±0.6	13.8±0.6	14.4±0.6	14.9±0.6
SB	9.8±0.5	9.1±0.5	9.1±0.5	9.5±0.5	9.7±0.5

VČ- Vrška Čuka anthracite, KL - Kostolac lignite, SB - Sokobanja brown coal

3. 3. Gas chromatography with flame ionization detection analyses

Certainly, the extraction/dissolution process leads to changes in the composition of organic matter, as new compounds (paraffins and olefins) are formed, as shown in Reactions (1) and (2).

$nCO + (2n+1)\ H_2 = nH_2O + C_nH_{2n+2}$ (paraffins) (1)

$nCO + 2nH_2 = nH_2O + C_nH_{2n}$ (olefins) (2)

Figure 4 and Table 3 show the formed compounds and their contents at the initial temperature in the study (373 K) as well as at the initial, middle and final time intervals [(a) 2 h, (b) 12 and (c) 20 h, Figure 4].

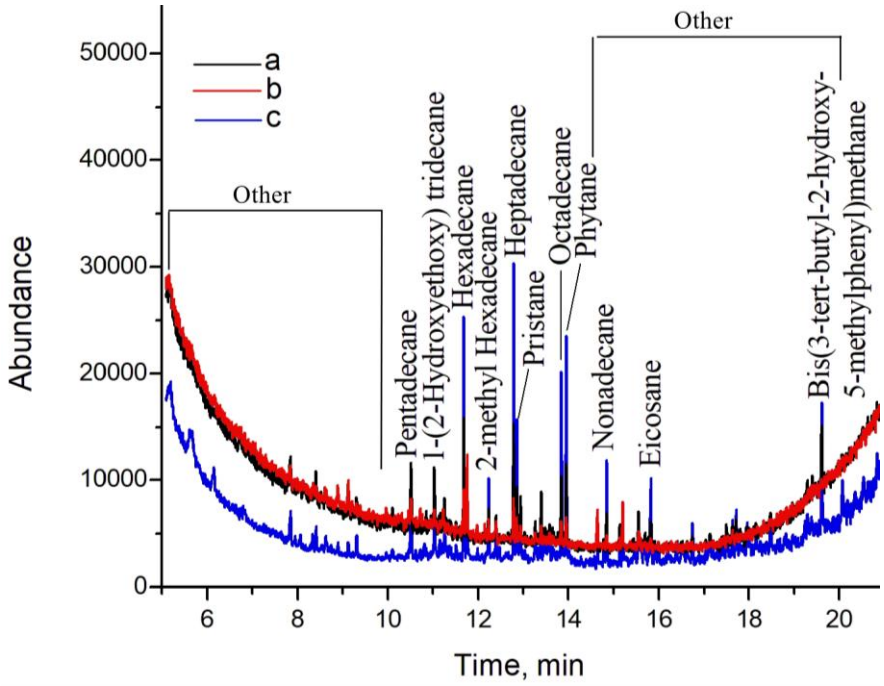

Figure 4. *GC/FID chromatograms of dissolved components obtained by heating the demineralized Vrška Čuka anthracite at 373 K (a-2 h, b-12 h and c-20 h)*

Table 3*. Mass percentage of extracted components in the solution phase from demineralized Vrška Čuka anthracite at 373 K at different extraction times*

No	Paraffins C_{12}-C_{19}	Formula	RI^{exp}	RI^{lit}	Method	Content, %		
						2 h	12 h	20 h
1.	Tridecane	$C_{13}H_{28}$	1298	1300	RI, MS	<1	<1	<1
2.	Tetradecane	$C_{14}H_{30}$	1398	1400	RI, MS	<1	<1	<1
3.	Pentadecane	$C_{15}H_{32}$	1498	1500	RI, MS	5	3	<1
4.	Hexadecane	$C_{16}H_{34}$	1599	1600	RI, MS	7	8	10
5.	2-Metyl-hexadecane	$C_{17}H_{36}$	1656	1666	RI, MS	5	5	6
6.	Heptadecane	$C_{17}H_{36}$	1698	1700	RI, MS	11	7	11
7.	Pristane	$C_{19}H_{40}$	1713	1704	RI, MS	6	11	7
8.	Octadecane	$C_{18}H_{38}$	1798	1800	RI, MS	8	8	9
9.	Nonadecane	$C_{19}H_{40}$	1898	1900	RI, MS	5	5	4
	Total paraffins C_{12}-C_{19}					48	48	50
	n-Paraffins	No.: 1-4,6,8, 9				39	38	37
	Terpenoid alkane	No.: 5, 7				12	13	13
	Other					1	1	<1
	Total identified					100	100	100

RI^{lit}-Retention indices from literature [27]; RI^{exp}: Experimentally determined retention indices using a homologous series of *n*-alkanes (C_8-C_{20} and C_{21}-C_{40}) on the HP-5MS column. MS: constituent identified by mass-spectra comparison; RI: constituent identified by retention index matching.

The total mass fraction of components after complete dissolution was determined by summing their individual mass fractions, which were calculated as the percentage of the soluble phase shown in Table 2. At this temperature, the proportion of newly formed paraffins (C_{12} to C_{19}), *n*-paraffins ($C_{1\text{-}4,\ 6,\ 8,\ 9}$) and terpenoid alkane remains relatively constant (Table 3). Olefins were not detected in any sample. Similar but not identical trends are observed in the contents of these compounds after 20 h of dissolution across all five temperatures (Table 4). Based on the presented results, the mass fraction of all formed paraffins remains relatively constant up to 423 K. At temperatures between 423 and 473 K, the

proportion of C_{12}-C_{19} paraffins increases, while that of *n*-paraffins ($C_{1\text{-}4,\ 6,\ 8,\ 9}$) decreases. The content of terpenoid alkane decreases slightly with increasing temperature. Also, olefins were not detected. These increases and decreases are within a range of ≤20 %.

***Table 4**. Mass percentage of extracted components in the solution phase from demineralized Vrška Čuka anthracite after 20 hours of dissolution at different temperatures*

No	Paraffins C_{12}-C_{19}	Formula	RI^{exp}	RI^{lit}	Method	Content, %				
						373 K	398 K	423 K	448 K	473 K
1.	Tridecane	$C_{13}H_{28}$	1298	1300	RI, MS	<1	<1	<1	1	2
2.	Tetradecane	$C_{14}H_{30}$	1398	1400	RI, MS	<1	<1	1	1	2
3.	Pentadecane	$C_{15}H_{32}$	1498	1500	RI, MS	<1	3	3	4	4
4.	Hexadecane	$C_{16}H_{34}$	1599	1600	RI, MS	10	9	9	10	10
5.	2-Metyl-hexadecane	$C_{17}H_{36}$	1656	1666	RI, MS	11	10	10	11	13
6.	Heptadecane	$C_{17}H_{36}$	1698	1700	RI, MS	6	8	8	8	9
7.	Pristane	$C_{19}H_{40}$	1713	1704	RI, MS	9	8	8	9	9
8.	Octadecane	$C_{18}H_{38}$	1798	1800	RI, MS	7	7	7	7	7
9.	Nonadecane	$C_{19}H_{40}$	1898	1900	RI, MS	4	5	5	5	5
Total paraffins C_{12}-C_{19}						50	51	51	56	61
n-Paraffins		No.: 1-4,6,8, 9				37	36	36	31	27
Terpenoid alkane		No.: 5, 7				13	12	12	12	11
Other						<1	1	1	1	1
Total identified						100	100	100	100	100

The composition of the soluble phase obtained during the extraction of Vrška Čuka anthracite was qualitatively and quantitatively compared with those obtained from demineralized lignite from Kostolac (57 % organic matter in coal) and brown coal from Sokobanja (64 % organic matter in coal), which are coals of lower maturity (Figure 5).

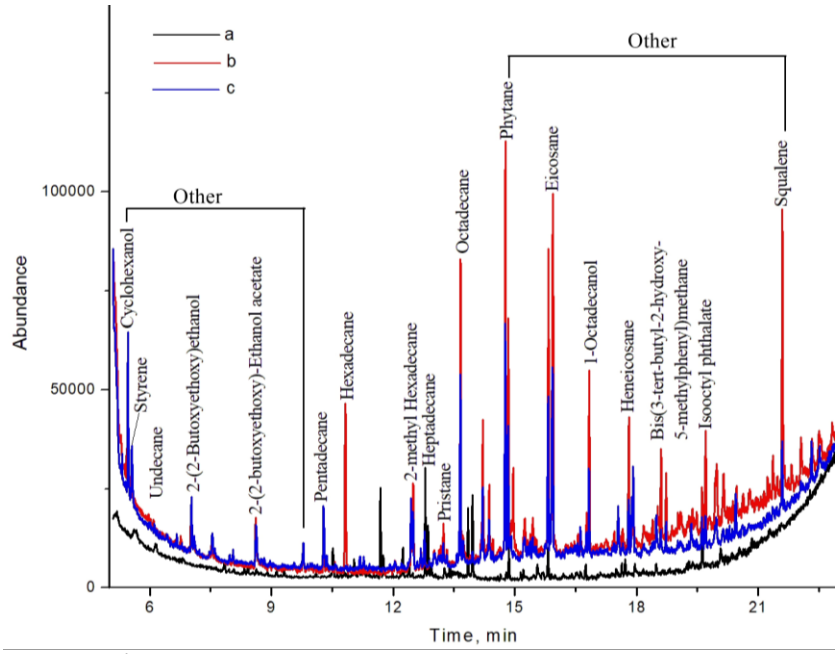

***Figure 5.** GC/FID chromatograms of soluble phases after 2 h of dissolution of demineralized (a) lignite, (b) brown coal and (c) anthracite*

The quantitative comparative results are presented in Table 5, where the soluble phases obtained after the first 20 h of dissolution at 373 K were selected, as they exhibited the highest mass percentages of the formed aliphatic compounds. It can be observed that with increasing coalification, the proportion of *n*-paraffins decreases, while the proportion of terpenes increases.

Figure 6 shows the mass spectra of the most abundant components after dissolution (20 h) at 373 K in the Vrška Čuka demineralized anthracite samples.

***Table 5**. Mass percentage of extracted components in the solution phase from demineralized anthracite, lignite, and brown coal after 20 h at 373 K*

No	Paraffins C_{12}-C_{19}	Formula	RI^{exp}	RI^{lit}	Method	Content (%)		
						KL	SB	VČ
1.	Tridecane	$C_{13}H_{28}$	1298	1300	RI, MS	<1	<1	<1
2.	Tetradecane	$C_{14}H_{30}$	1398	1400	RI, MS	<1	<1	<1
3.	Pentadecane	$C_{15}H_{32}$	1498	1500	RI, MS	<1	2	<1
4.	Hexadecane	$C_{16}H_{34}$	1599	1600	RI, MS	25	22	10
5.	2-Metyl-hexadecane	$C_{17}H_{36}$	1656	1666	RI, MS	27	19	11
6.	Heptadecane	$C_{17}H_{36}$	1698	1700	RI, MS	6	8	8
7.	Pristane	$C_{19}H_{40}$	1713	1704	RI, MS	<1	2	9
8.	Octadecane	$C_{18}H_{38}$	1798	1800	RI, MS	<1	3	7
9.	Nonadecane	$C_{19}H_{40}$	1898	1900	RI, MS	<1	2	4
	Total paraffins C_{12}-C_{19}					54	53	49
	n-Paraffins	No.: 1-4,6,8, 9				45	43	47
	Terpenoid alkane	No.: 5, 7				1	4	13
	Other					<1	<1	<1
	Total identified					100	100	100

KL - Kostolac lignite, SB - Sokobanja brown coal, VČ - Vrška Čuka anthracite

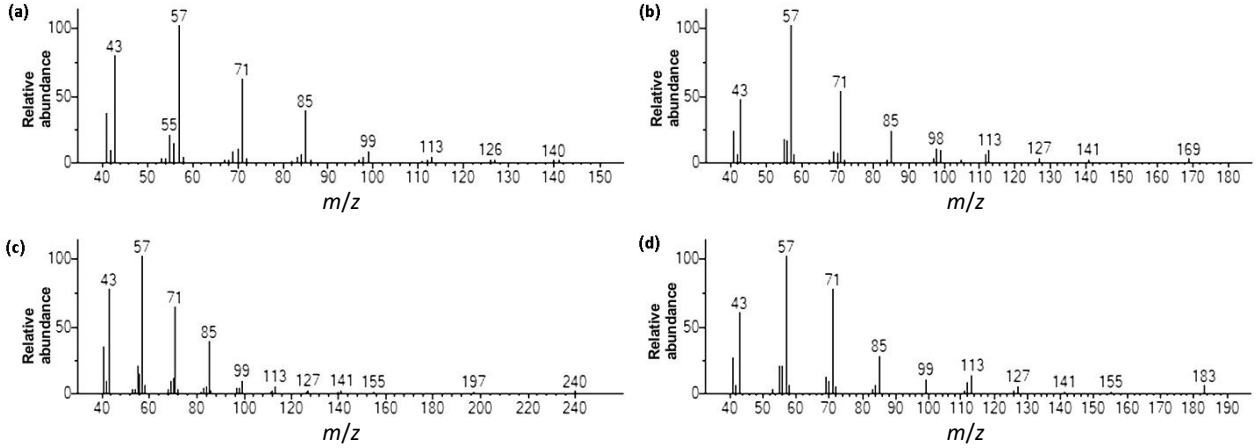

***Figure 6.** Mass spectra of the most abundant components after dissolution (20 h) at 373 K in the Vrška Čuka demineralized anthracite samples: (a) hexadecane, (b) 2-methyl hexadecane, (c) heptadecane and (d) pristane*

3. 4. Fourier transform infrared spectroscopy analysis

The present study of organic matter from Vrška Čuka anthracite confirms a high concentration of aromatic hydrocarbons and a minor amount of aliphatic hydrocarbons [15,16]. After 2 hours of extraction at 473 K, methyl groups (CH_3) with an absorption peak at 2972 cm^{-1} were extracted/removed from the organic residue (Figure 7). These methyl groups are likely those independently bound within the macromolecular structure of the coal-derived organic matter. In contrast, ethyl groups (CH_2) in the chain (absorption peaks at 2924, 2852, and 1377 cm^{-1}) remained unchanged. Further extraction revealed that after 20 hours, the complete removal of aliphatic compounds occurred (*i.e.* in addition to CH_3 groups, CH_2 groups also disappeared, as indicated by the absence of aliphatic structures in the 2960 to 2860 cm^{-1} region). The peak at ~1692 cm^{-1} is characteristic of the carbonyl (C=O) stretching vibration. This peak, along with the peak at 1635 cm^{-1} (attributed to conjugated C=C bonds), remained unchanged. Peaks at approximately 1585 and 1455 cm^{-1} originate from carboxylic group -COO- [28]. Similarly, changes were not observed in these peaks or in the peaks of aromatic structures in the 880 to 770 cm^{-1} region.

Recently, Zheng *et al.* [29] investigated the low-temperature oxidation of anthracite, as well as the stability of its aliphatic structures. The temperatures applied in their experiments (253 to 423 K), correspond to the temperatures of SHWV used in our study over similar time intervals.

Their results demonstrated that aliphatic moieties located within the interlayer space of the organic matrix are more stable than those situated at its periphery. In contrast to their approach, our method showed that the application of SHWV

leads to the complete detachment of aliphatic structures from the organic residue already at 373 K. A common feature of both approaches is the discontinuous behaviour observed in the stability of aliphatic structures within the samples.

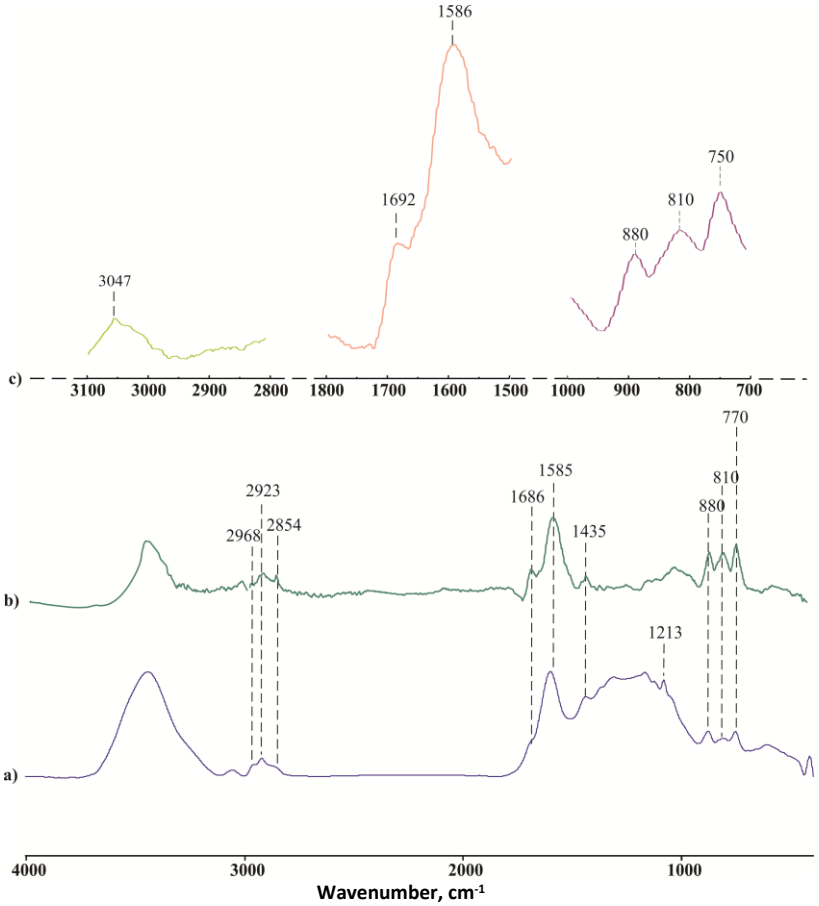

Figure 7. *FTIR spectra of anthracite from Vrška Čuka: a) initial demineralized sample, b) residue after 2 hours of extraction and c) residue after 20 hours of extraction at 473 K*

To compare different coals, FTIR spectra of the organic matter and the organic residue remaining after 2 hours of extraction from Sokobanja brown coal and Kostolac lignite are also presented (Figures 8 and 9, respectively).

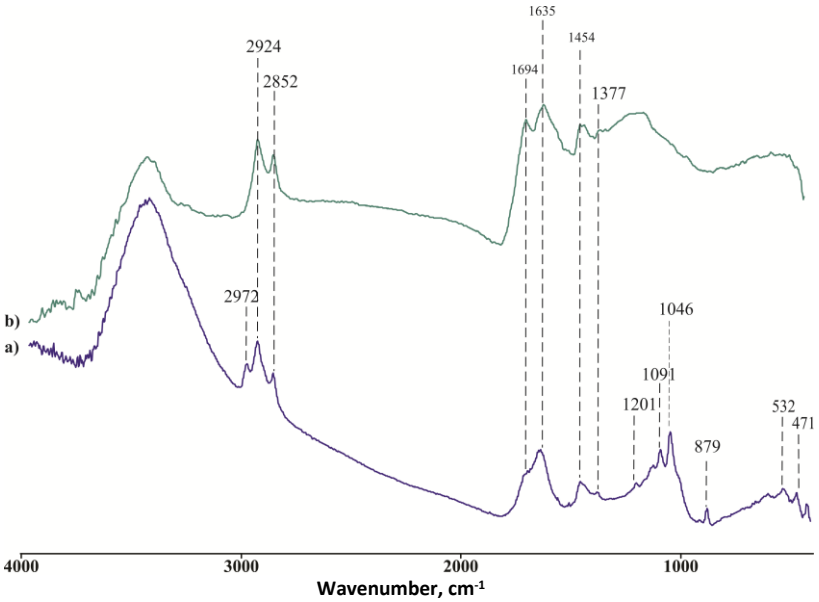

Figure 8. *FTIR spectra of brown coal from Sokobanja: a) initial demineralized sample and b) residue after 2 hours of extraction at 473 K*

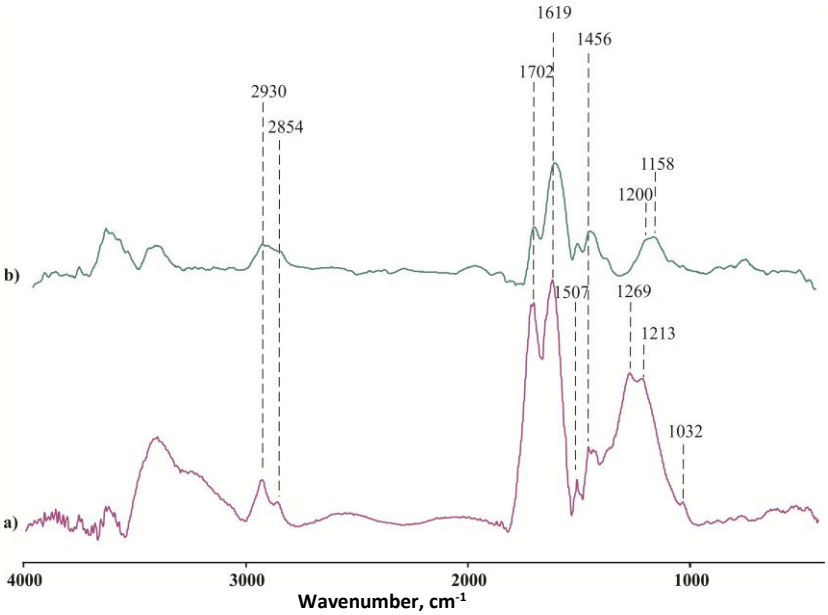

Figure 9. *FTIR spectra of lignite from Kostolac: a) initial demineralized sample and b) residue after 2 hours of extraction at 473 K*

In the case of the organic matter in Sokobanja brown coal, a broad band around 3400 cm^{-1} represents physically adsorbed water. Here, the loss of CH_3 groups, indicated by the disappearance of the absorption peak at 2972 cm^{-1}, likely corresponds to methyl groups that were present as side chains or isolated substituents on the macromolecular structure. In contrast, CH_2 groups in the chain (absorption peaks at 2924, 2852 and 1377 cm^{-1}) remained unchanged. Small peaks at 1201, 1091 and 1046 cm^{-1} originate from C-O and C-O-C bonds of alcohols, hydrogen peroxide and ethers. These peaks disappeared after extraction, along with peaks below 1000 cm^{-1}, attributed to C=C-H. Peaks at 1694 cm^{-1}, 1585 cm^{-1} and 1456 cm^{-1} remained unchanged. These two coals are compared because they are from the same area, but of different maturities.

4. CONCLUSION

Thermal solubility experiments performed in the present study show that the solubility rate of organic matter from demineralized anthracite from Vrška Čuka (Serbia) is highest during the first two hours of extraction. FTIR analysis reveals that during these initial 2 hours at all investigated temperatures, there is a loss of methyl groups, likely present as side chains attached to aromatic rings in the organic matrix. In the subsequent hours of dissolution, gradual degradation of ethyl groups occurred, leading to their complete removal after 20 hours. In lignite and brown coal samples, ethyl groups are also gradually removed during extraction, while methyl groups are either absent or present only in minor amounts.

The extracted solutions from demineralized anthracite from Vrška Čuka, obtained at extraction temperatures up to 423 K, show almost constant stable mass fractions of all paraffins. With further increases in the extraction temperature up to 473 K, the proportion of C_{12}-C_{19} paraffins increases, while the proportion of *n*-paraffins ($C_{1\text{-}4,\ 6,\ 8,\ 9}$) decreases reciprocally. In all analyses, the extracted solutions from anthracite showed stable terpene content, whereas the compared lignite and brown coal samples exhibited an increase in terpene levels. This difference can be attributed to their respective stages of coalification: anthracite is highly mature (metagenesis), while brown coal and lignite are less mature and remain in the diagenesis stage.

The results of this study demonstrate that the extraction method employed is effective for the quantitative extraction and separation of both short- and long-chain aliphatic hydrocarbons from the coal organic matter. Analysis of the extraction yield of aliphatic hydrocarbons enables the selection of the most suitable SHWV temperature for quantitative extraction, depending on the intended application, and provides insight into the method's potential uses.

Acknowledgements: *This work was supported by the Ministry of Science, Technological Development and Innovation of the Republic of Serbia (Financing program for scientific research work, No: 451-03-137/2025-03/200133).*

REFERENCES

[1] Whiteside JH, Olsen PE, Eglinton T, Brookfield ME, Sambrotto RN. Compound-specific carbon isotopes from Earth's largest flood basalt eruptions directly linked to the end-Triassic mass extinction. *PNAS.* 2010; 107(15): 6721-6725. https://doi.org/10.1073/pnas.10017061

[2] Vail PR, Mitchum RMJR, Thompson S. Seismic stratigraphy and global changes in sea level. In: *Seismic Stratigraphy Application to Hydrocarbon Exploration*, Payton C, Ed., AAPG Mem; 1977: 127-135. https://doi.org/10.1306/M26490C3

[3] Haq BU., Hardenbol J, Vail PR. Chronology of fluctuating sea levels since the Triassic. *Science*, 1987; 235: 1156-1167. https://doi.org/10.1126/science.235.4793.115

[4] Golonka J, Krobicki M. Jurassic paleogeography of the Pieniny and Outer Carpathian basins. *Riv. Ital. Paleontol. Strat.* 2004; 110: 5–14. https://doi.org/10.13130/2039-4942/6252

[5] Schmid SM, Bernoulli D, Fügenschuh B, Matenco L, Schefer S, Schuster R, Tischler M, Ustaszewski K. The Alpine-Carpathian-Dinaridic orogenic system: correlation andevolution of tectonic units. *Swiss J Geosci*. 2008; 101: 139-183. https://doi.org/10.1007/s00015-008-1247-3

[6] Veselinović M, Antonijević I, Lončarević Č, Kalenić M, Rajčević D, Krstić B, Banković V, Rakić B. *Geological map of the SFR Yugoslavia, Sheet Zaječar 1:100.000*. Belgrade: Savezni Geološki zavod; 1967.

[7] Veselinović D. Dobra on Danube: Vrška Čuka. In: Petković K. ed. *Geology of Serbia. II-2. Stratigraphy, Mesozoic.* Faculty of Mining and Geology, University of Belgrade. 1975; 73-75. (in Serbian). COBISS.CG-ID - 21709327

[8] Andjelković M, Mitrović-Petrović J, Jankičević J, Rabrenović D, Andjelković J, Radulović V. Geology of Stara planina: Stratigraphy Faculty of Mining and Geology, Institute for Regional Geology and Palaeontology, University of Belgrade, 1996; p. 247 (in Serbian). COBISS-ID: 47775500

[9] Tchoumatchenco P, Rabrenović D, Radulović V, Malešević N, Radulović B. Trans-border (north-east Serbia/north-west Bulgaria) correlations of the Jurassic lithostratigraphic units. *Ann Géol Pénins Balk.* 2011; 72: 1-20. https://doi.org/10.2298/GABP1172001T

[10] Akinlua A, Smith RM. High Temperature Steam Extraction for the Determination of Aliphatic Hydrocarbons in Petroleum Source Rock. *Chroma*. 2009; 69: 1333-1339. https://doi.org/10.1365/s10337-009-1057-4

[11] Monin JC, Barth D, Perrut M, Espitalié M, Durand B. Extraction of hydrocarbons from sedimentary rocks by supercritical carbon dioxide. *Org Geochem*. 1988; 13: 1079-1086. https://doi.org/10.1016/0146-6380(88)90292-6Get rights and content

[12] Greibrokk T, Radke M, Skurdal M, Willsch H. Multistage supercritical fluid extraction of petroleum source rocks: application to samples from Kimmeridge clay and Posidonia Shale formations. *Org Geochem*. 1992; 18: 447-455. https://doi.org/10.1016/0146-6380(92)90107-9

[13] Yao C, Hou Y, Sun Y, Wu W, Ren S, Liu H. Extraction of aromatics from aliphatics using a hydrophobic dicationic ionic liquid adjusted with small-content water. *Sep Purif Technol*. 2020; 236: 116287. https://doi.org/10.1016/j.seppur.2019.116287

[14] Nematollahi H, Moradi N, RiyaziNejad M, Vahidi H. Removal of Aliphatic Hydrocarbons from Gas Oil Contaminated Clay Soil via Soil Vapor Extraction. *Civ Eng J*. 2018; 4(8): 1858. http://dx.doi.org/10.28991/cej-03091120

[15] Premović PI. Organic free radicals in Precambrian and Paleozoic rocks: origin and significance. In: *Early Organic Evolution: Implications for Mineral and Energy Resources,* Schidlowski M, ed., Springer-Verlag, Berlin; 1992: 241-256. https://doi.org/10.1007/978-3-642-76884-2_18

[16] Juma A, Todorović B, Stojiljković D, Nikolić Lj, Petrović-Pantić T, Premović PI. Polyaromatic structure in the kerogen from anthracite at Vrška Čuka (Carpatho-Balkan region, Serbia). *Adv Technol*. 2023; 12(1): 38-43. https://doi.org/10.5937/savteh2301038J

[17] Zhang L, Hu S, Xu K, Jiang, L Wang Y, Su S, Xiao Y, Shan L, Shen W, Li H, Chen G, Xiang J. Study on the structural evolution of semi-chars and their solvent extracted materials during pyrolysis process of a Chinese low-rank coal. *Fuel*. 2018; 214: 363-368. https://doi.org/10.1016/j.fuel.2017.11.043.

[18] Vindušková O, Sebag D, Cailleau G, Brus J, Frouz J, Methodological comparison for quantitative analysis of fossil and recently derived carbon in mine soils with high content of aliphatic kerogen. *Org Geochem*. 2015; 89-90: 14-22. https://doi.org/10.1016/j.orggeochem.2015.10.001.

[19] Khalekuzzaman M, Sharif Jemi T, Chowdhury D, Nasim K, Nafis Pantho, Md. Islam, Advancing hydrothermal liquefaction: Best solvents for aliphatic-rich biocrude extraction from fecal sludge, *J Environm Chem Eng.* 2025; 13(2): 115959. https://doi.org/10.1016/j.jece.2025.115959.

[20] Wolbach WS, Andres E. Elemental carbon in sediments: Determination and isotopic analysis in the presence of kerogen. *Geochim Cosmochim Acta*. 1989; 53: 1637-1647. https://doi.org/10.1016/0016-7037(89)90245-7

[21] Lüning SDK, Loydell DK, Sutcliffe O, Ait Salem A, Zanella E, Craig J, Harper DAT. Silurian-lower Devonian black shales in Morocco: which are the organically richest horizons? *J Pet Geol*. 2000; 23: 293-311. https://doi.org/10.1111/j.1747-5457.2000.tb01021.x

[22] Premović PI, Allard T, Nikolić ND, Tonsa IR, Pavlović MS. Estimation of vanadyl porphyrins concentration in sedimentary kerogens and asphaltenes. *Fuel*. 2000; 79(7): 813-819. https://doi.org/10.1016/S0016-2361(99)00205-7
[23] Software Informer. AMDIS 2.7. https://amdis.software.informer.com/2.7/
[24] Wiley Science Solutions. GC-MS Spectral Databases. https://sciencesolutions.wiley.com/solutions/technique/gc-ms/
[25] NIST Standard Reference Database 1A. https://chemdata.nist.gov/mass-spc/ms-search/docs/Ver20Man_11.pdf
[26] Agilent. Libraries for GC/MSD. https://www.agilent.com/en/product/gas-chromatography-mass-spectrometry-gc-ms/gc-ms-application-solutions/gc-ms-libraries
[27] NIST Chemistry WebBook, NIST Standard Reference Database Number 6, National Institute of Standards and Technology https://doi.org/10.18434/T4D303
[28] Rahman ZU, Xianshu D. Study on Improving Flotation Effect and Mechanism of Fine Anthracite by Polyacrylamide, Sodium Silicate and Sodium Oleate. *EJTAS*. 2023; 1(4): 197-210. https://orcid.org/0009-0004-8399-7308
[29] Zheng Q, Huang B, Liu S, Song X, Shi S. Influence of aliphatic species on coal molecular structure during low-temperature oxidation of anthracite coal. *Environ Process.* 2020; 7:159-171. https://doi.org/10.1007/s40710-019-00411-9

Ekstrakcija alifatičnih ugljovodonika iz demineralizovanog antracita sa lokaliteta Vrška Čuka (Srbija) pregrejanom vodenom parom na različitim temperaturama

Amer M. Juma[1], Ljubiša B. Nikolić[1], Bratislav Ž. Todorović[1], Jelena S, Stanojević[1], Snežana S. Trifunović[2], Tanja Petrović Pantić[3] i Sanja M. Petrović[1]

[1]Tehnološki fakultet, Univerzitet u Nišu, Leskovac, Srbija
[2]Hemijski fakultet, Univerzitet u Beogradu, Beograd, Srbija
[3]Geološki zavod Srbije, Beograd, Srbija

(Naučni rad)

Izvod

Ekstrakcija alifatičnih ugljovodonika pregrejanom vodenom parom iz organskih ostataka uglja predstavlja perspektivnu metodu zbog smanjenja industrijskih troškova potrebnih za njihovo dobijanje. U ovom radu ekstrakcija je izvedena u opsegu temperatura bez prisustva katalizatora (373 do 473 K; 2-20 h). Najveći prinos izdvojene organske materije ostvaren je tokom prva 2 h (4,0 do 6,1 % početne mase uzorka). Pri dužim vremenima, vrednosti rastvorljivosti su varirale, što ukazuje da oslobađanje alifatičnih ugljovodonika zavisi od njihovog položaja u različitim strukturnim domenima organske matrice. Visok stepen zrelosti organske materije ukazuje da je uzorak antracita u fazi metageneze. Gasna hromatografija sa plameno-jonizacionom detekcijom pokazala jeda ekstrakcija do stvaranja n-parafina, prvenstveno energetski značajnih homologa C12 do C19, koji čine 50 do 61 % izdvojenih jedinjenja nakon 20 sati. Poređenje sa manje zrelim ugljevima (lignit i mrki ugalj) iz istog područja je pokazalo sličnu tendenciju, ali sa povećanjem ugljenifikacije/sazrevanja, udeo n-parafina se smanjuje, dok se udeo terpena povećava. Infracrvena spektroskopija sa Furijeovom transformacijom suvog ostatka nakon ekstrakcije pokazala je da su metil-grupe (2972 cm^{-1}) nestale nakon 2 sata na svim temperaturama, dok je potpuna eliminacija alifatičnih struktura, uključujući etil-grupe (2924, 2852 i 1377 cm^{-1}), zabeležena nakon 20 sati. Detektovani parafini i terpeni potiču od metil- i etil-grupa ekstrahovanih iz organskog ostatka uglja. Dodatno, iako su lignit i mrki ugalj dali gotovo identične rezultate, u lignitu nisu detektovane nezavisno vezane metil-grupe.

Ključne reči: ugalj, rastvorljivost, sazrevanje, parafini, metil grupe

Science and arts intertwined: Defend knowledge, defend with knowledge

Bojana M. Obradović

University of Belgrade, Faculty of Technology and Metallurgy, Belgrade, Serbia

Abstract

Events that combine scientific and artistic exhibitions in public spaces are rare, yet they offer a unique opportunity to present diverse perspectives on how we experience, interpret, and express our understanding of the world. "Defend Knowledge, Defend with Knowledge," held on June 6 in Belgrade, Serbia, transformed Students' Square into a vibrant venue featuring interactive scientific presentations, topical discussions, and artistic showcases by members of the University of Belgrade and the University of Arts in Belgrade, two institutions that play a vital role in Serbia's academic, cultural, and social life. Visitors engaged with state-of-the-art topics in natural and technical sciences, participated in hands-on activities for children, and attended sessions on educational fairness, emotional intelligence, and lifelong learning. Artistic displays, including a charity bazaar, student film screenings, and musical performances, further enriched the event's atmosphere. More than just informing and entertaining, the event conveyed a powerful message: universities are inextricably linked to society, working to improve life and the environment while offering solutions to contemporary challenges. By sharing scientific and artistic achievements in a common space, the event fostered curiosity, dialogue, and a sense of community, highlighting the essential role of knowledge and culture in society.

Keywords: University of Belgrade; University of Arts in Belgrade; interdisciplinary collaboration; public engagement; societal challenges; higher education.

Available on-line at the Journal web address: http://www.ache.org.rs/HI/

BOOK AND EVENT REVIEW

Hem. Ind. **80(2)** 107-11 (2026)

1. INTRODUCTION

There are few events globally that combine scientific and artistic exhibitions, despite the appeal of presenting diverse perspectives on how we experience, interpret, and express our understanding of the world around us. While there are a few well-known international examples of science and art festivals or galleries, most of them focus on in-depth collaborations between scientists and artists or feature curated science-art exhibitions. The event "Defend Knowledge, Defend with Knowledge" held on June 6 in Belgrade, Serbia, offered a different but equally valuable approach: an open, street-level exhibition that brought together interactive scientific presentations, topical discussions, and artistic showcases from members of the University of Belgrade and the University of Arts in Belgrade.

Both universities play a vital role in the academic, cultural, and social life of Serbia. The University of Belgrade, established nearly 220 years ago, is the oldest and most significant academic institution in Serbia and the region. With 31 faculties and 11 research institutes spanning the social sciences, humanities, medical sciences, natural sciences, and engineering, it is recognized as a higher education institution of national importance. The University of Belgrade ranks among the top 1.9 % of universities worldwide according to the 2025 Global 2000 list by the Center for World University Rankings [1] and is consistently listed among the top 500 universities globally by the Academic Ranking of World Universities (ARWU) [2].

Equally significant is the University of Arts in Belgrade, comprising four faculties: Music, Fine Arts, Applied Arts, and Dramatic Arts. Although founded in 1957, its roots extend to the 19th century, with university-level arts education beginning in 1937 with the Academy of Fine Arts and the Music Academy, followed by the School of Applied Art in 1938. The University of Arts has profoundly shaped the cultural and artistic landscape of Serbia and the wider region, with many of the most eminent artists serving as educators and mentors.

Corresponding author: Bojana Obradović; E-mail: bojana@tmf.bg.ac.rs, https://orcid.org/0000-0002-7276-0442,
University of Belgrade, Faculty of Technology and Metallurgy, Karnegieva 4, Belgrade, Serbia
Paper received: 26 July 2025; Paper accepted: 24 August 2026; Paper published: 31 August 2026.

The event on June 6 represented only a glimpse of the broad impact these universities have on Serbian society and beyond. Among the highlights, the Faculty of Biology, Faculty of Technology and Metallurgy, Faculty of Physics, Faculty of Physical Chemistry, and the Institute of Chemistry, Technology and Metallurgy presented a diverse array of state-of-the-art topics in natural and technical sciences relevant to modern society (Figure 1). Passersby could learn about wastewater treatment, the transformation of various waste types into useful products and energy, novel biomaterials and advanced 3D-printed implants for dentistry and orthopedics, the advantages and disadvantages of lithium-ion versus sodium-ion batteries, genetic screening tests, climate change, and the use of planktonic organisms as indicators of environmental disturbances in aquatic systems. Alongside these "serious topics," the exhibitions featured interactive experiments for children, who could create colorful jelly worms from alginate hydrogels, make batteries and bath bombs, observe algal cells under a microscope, and take a quiz on scientific names for various animals. Together, these topics and hands-on activities highlighted not only the relevance and impact of scientific research on society, but also the joy of discovery for all ages.

***Figure 1**. Highlights from the natural and technical sciences exhibition*

In addition to the natural and technical sciences, the event also offered a space for reflection on the social and humanistic dimensions of knowledge. The Faculty of Philosophy contributed interactive sessions exploring questions of fairness in education, the role of learning in times of social change, the importance of emotional intelligence, and perspectives on adult education (Figure 2). These thought-provoking discussions invited participants to reflect on contemporary challenges in society and personal development from a humanistic angle.

Figure 2. *Interactive exhibition on emotional intelligence: "(Don't) Play with Feelings! A Little Bit about Emotional Intelligence :)" ("(Ne) igraj se osećanjima! Nešto malo o emocionalnoj inteligenciji :)")*

However, the aim of the event was not only to inform, educate, entertain, and engage passersby, but also to convey a powerful message: universities are an inextricable part of society, dedicated to improving all aspects of life and the environment and providing solutions to contemporary challenges. In this spirit, the event featured an interdisciplinary interactive exhibition on two controversial mining projects in the Jadar and Homolje regions of Serbia. Both projects have raised nationwide concerns about toxic pollution, habitat destruction, and water contamination. Passersby had the opportunity to receive in-depth scientific information and engage directly with experts from the University of Belgrade. Additionally, a panel on university autonomy brought together six panelists from both participating universities to discuss the current status of universities in Serbia and the importance of maintaining autonomy for society as a whole (Figure 3). The discussion offered a historical perspective and emphasized that universities serve as early-warning systems for societal, economic, and ecological crises.

Figure 3. *Panel on university autonomy (from left to right): Prof. Dejan Šabić (Faculty of Geography, UB), Prof. Katarina Popović (Faculty of Philosophy, UB), Prof. Dejan Pavlović (Faculty of Political Science, UB), Prof. Katarina Jovanović (Faculty of Music, UAB), Prof. Aleksandar Baucal (Faculty of Philosophy, UB), and Dr. Adriana Zaharijević (Institute for Philosophy and Social Theory, UB). (UB – University of Belgrade; UAB – University of Arts in Belgrade)*

Throughout the dynamic day, the scientific exhibitions and activities were interwoven with a range of artistic displays and programs. The Faculty of Applied Arts, Faculty of Dramatic Arts, and the Faculty of Music organized a charity bazaar featuring artistic crafts, artworks, and books by their own authors. The Faculty of Dramatic Arts also screened student films at its booth, while the Faculty of Music presented a rich program titled “All for Music, Music for All,” which featured student performances combining flute and electronics, as well as recitals by distinguished faculty members, including an acclaimed opera singer and exceptional pianists (Figure 4).

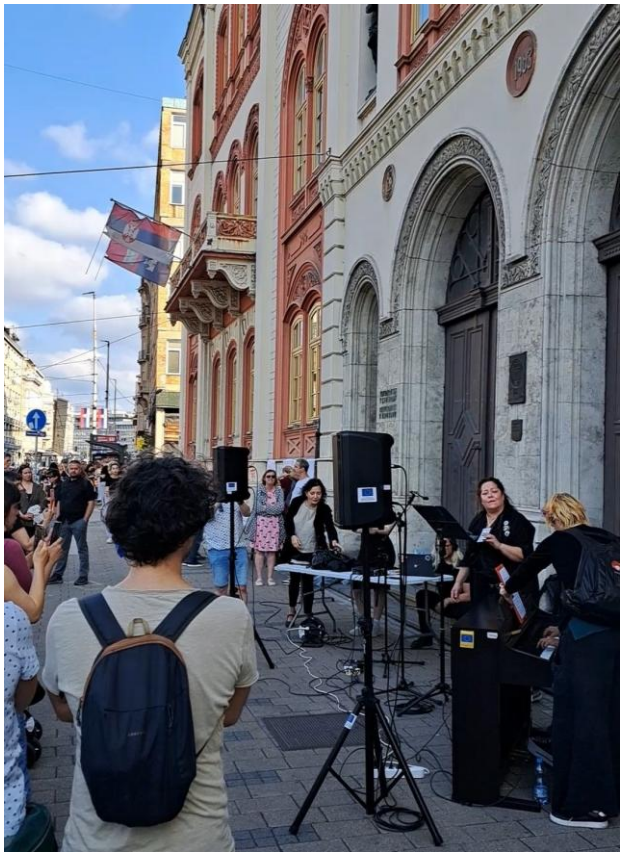

Figure 4. *Artistic performance of Serbian solo songs by Prof. Katarina Jovanović (soprano) and Zorka Milivojević (piano), Faculty of Music, University of Arts in Belgrade*

Overall, at the bustling Studentski trg (Students' Square) in front of the University of Belgrade Rectorate, the event attracted a steady stream of passersby and brought a vibrant spark to the city's usual Saturday rhythm. It demonstrated the power of sharing scientific and artistic achievements in a common space, inspiring curiosity, dialogue, and a sense of community around knowledge and creativity. In times when the value of knowledge and culture must be actively defended, such initiatives are more important than ever. We look forward to building on this success and seeing even more engagement at the next event in 2027!

REFERENCES

[1] Global 2000 list by the center for world university rankings, Center for World University Rankings, https://cwur.org/2025.php. Accessed June 20, 2026.
[2] Academic Ranking of World Universities (ARWU) 2025, Shanghai Ranking. https://www.shanghairanking.com/rankings/arwu/2025. Accessed June 20, 2026.

Susret nauke i umetnosti: Branimo znanje(m)

Bojana M. Obradović

Univerzitet u Beogradu, Tehnološko-metalurški fakultet, Beograd, Srbija

(Prikaz knjiga i događaja)

Izvod

Događaji koji prikazuju u javnom prostoru zajedno naučne i umetničke postavke su retki, ali nude jedinstvenu mogućnost predstavljanja različitih perspektiva o svetu koji nas okružuje. Postavka „Branimo znanje(m)", održana 6. juna u Beogradu, pretvorila je Studentski trg u živopisno mesto sa interaktivnim naučnim prezentacijama, tematskim diskusijama i umetničkim programima u kojima su učestvovale članice Univerziteta u Beogradu i Univerziteta umetnosti u Beogradu, dve institucije koje imaju ključnu ulogu u akademskom, kulturnom i društvenom životu Srbije. Prolaznici su imali priliku da se upoznaju sa savremenim temama iz prirodnih i tehničkih nauka, učestvuju u interaktivnim radionicama za decu, kao i na sesijama o pravičnosti obrazovanja, emocionalnoj inteligenciji i učenju tokom celog života. Umetnički programi, uključujući humanitarni bazar, projekcije studentskih filmova i muzičke nastupe, dodatno su obogatili atmosferu događaja. Pored informativnih i zabavnih aktivnosti, poslata je i važna poruka: univerziteti su neraskidivo povezani sa društvom i posvećeni poboljšanju kvaliteta života i životne sredine, nudeći rešenja za sve savremene izazove. Kroz zajedničko predstavljanje naučnih i umetničkih dostignuća, događaj je podstakao radoznalost, dijalog i osećaj zajednice, naglašavajući ključnu ulogu znanja i kulture u društvu.

Ključne reči: Univerzitet u Beogradu; Univerzitet umetnosti u Beogradu; interdisciplinarna saradnja; uključivanje javnosti; izazovi današnjice; visoko obrazovanje

Представљање монографије „Hydrodynamics and Mass Transfer of Multiphase Reciprocating Plate Columns“

Ивана Т. Дрвеница

Универзитет у Београду, Институт за медицинска истраживања, Београд, Србија

Извод

У конференцијској сали компаније ДЦП Хемигал у Лесковцу 23. априла 2026. године одржана је промоција монографије “Hydrodynamics and Mass Transfer of Multiphase Reciprocating Plate Columns”, аутора академика Владе Б. Вељковића, проф. др Иване Б. Банковић Илић и проф. др Дејана У. Скале. Монографију је 2025. године објавио Огранак Српске академије наука и уметности у Нишу.

Кључне речи: хемијско инжењерство, вишефазни системи, колона са вибрационом мешалицом

Доступно он-лине на веб адреси часописа: http://www.ache.org.rs/HI/

ВЕСТИ

*Hem. Ind.***80(2)** 113-115 (2026)

Монографија “Hydrodynamics and Mass Transfer of Multiphase Reciprocating Plate Columns” представља значајан допринос области хемијског инжењерства и резултат је вишедеценијског научноистраживачког рада наших истраживача у области вишефазних система, посебно колона са вибрирајућом мешалицом (енгл. reciprocating plate columns). Ови контактни апарати имају важну примену у вишефазним процесима, као што су екстракције течност-течност и апсорпције гас-течност, затим у биопроцесима и савременим технологијама интензификације процеса.

Слика 1.Аутори и учесници промоције монографије „Hydrodynamics and Mass Transfer of Multiphase Reciprocating Plate Columns“, компанија „ДЦП Хемигал“, Лесковац, 23. април 2026. године

Figure 1. Authors and participants at the promotion of the monograph “Hydrodynamics and Mass Transfer of Multiphase Reciprocating Plate Columns”, DCP Hemigal, Leskovac, 23 April 2026.

(Слика преузета са https://www.ogranaknis.sanu.ac.rs/promocija-monografijehydrodynamics-and-mass-transfer-of-multiphase-reciprocating-plate-columns/)

Аутор за кореспонденцију: Ивана Т. Дрвеница, E-mail: ivana.drvenica@imi.bg.ac.rs https://orcid.org/0000-0003-4985-1642, Институт за медицинска истраживања, Универзитет у Београду, Србија,

Књига систематично обједињује фундаменталне принципе хидродинамике и преноса масе, експерименталне резултате, развој модела и корелација, као и инжењерске примене ових колона у различитим процесним технологијама. Посебна вредност монографије огледа се у томе што представља свеобухватан приказ развоја једне истраживачке области у Србији током више од педесет година и њеног доприноса развоју међународне научне заједнице.

Током промоције истакнуто је да ова публикација представља драгоцену референтну публикацију за истраживаче, наставнике, студенте докторских студија и инжењере који се баве транспортним појавама, сепарационим процесима, реакционим инжењерством и пројектовањем вишефазних система. Аутори су указали на значај континуираног развоја ове области и потребу за повезивањем фундаменталних истраживања са индустријским применама.

Промоција је окупила представнике академске заједнице, научноистраживачких институција и привреде, који су указали на значај очувања и промоције научних достигнућа српске школе хемијског инжењерства. Посебно је наглашена улога монографија као трајног извора знања и основе за даљи развој нових генерација истраживача.

Академик Влада Б. Вељковић, један од аутора монографије, тренутни је председник Савеза хемијских инжењера Србије (СХИ), а од 2007. године главни је и одговорни уредник часописа *Chemical Industry & Chemical Engineering Quarterly* (*CI&CEQ*) који издаје СХИ. Проф. др Дејан У. Скала, такође један од аутора, био је председник СХИ од 2016. до 2025. године, и главни и одговорни уредник часописа Хемијска индустрија (1994.-2005.) и *CI&CEQ* (2005.-2007.). Њихов дугогодишњи рад имао је и наставља да има значајну улогу у развоју, повезивању и афирмацији хемијског инжењерства у Србији. Проф. др Ивана Банковић Илић је подручни уредник часописа Хемијска индустрија и главни и одговорни уредник часописа *Advanced Technologies* (издавач: Технолошки факултет у Лесковцу), као и председник подружнице СХИ у Лесковцу.

Објављивањем монографије "*Hydrodynamics and Mass Transfer of Multiphase Reciprocating Plate Columns*", документован је битан део научног развоја области вишефазних система и додатно потврђен допринос српских истраживача савременом хемијском инжењерству.

Promotion of the monograph „Hydrodynamics and Mass Transfer of Multiphase Reciprocating Plate Columns“

Ivana T. Drvenica

University of Belgrade, Institute for Medical Research, Belgrade, Serbia

Abstract

The monograph “Hydrodynamics and Mass Transfer of Multiphase Reciprocating Plate Columns”, authored by Academician Prof. Dr. Vlada B. Veljković, Prof. Dr. Ivana B. Banković Ilić, and Prof. Dr. Dejan U. Skala, was promoted on April 23, 2026, in the conference hall of the company DCP Hemigal in Leskovac. The monograph was published in 2025 by the Niš Branch of the Serbian Academy of Sciences and Arts (SASA).

Keywords: chemical engineering; multiphase systems; reciprocating plate column.

NEWS

The monograph **“**Hydrodynamics and Mass Transfer of Multiphase Reciprocating Plate Columns**”** represents a significant contribution to the field of chemical engineering and is the result of decades of scientific research by Serbian scientists in the area of multiphase systems, particularly reciprocating plate columns. These contactors have found important applications in liquid–liquid extraction, gas–liquid contacting, bioprocesses, and modern process intensification technologies.

The book provides a comprehensive overview of the fundamental principles of hydrodynamics and mass transfer, experimental investigations, modelling approaches, correlations, and engineering applications of reciprocating plate columns. A key strength of the monograph is its comprehensive account of the development of this research field in Serbia over more than five decades and its contribution to the international scientific community.

During the promotion, it was emphasized that the monograph serves as an important reference for researchers, academics, doctoral students, and engineers working in the fields of transport phenomena, separation processes, reaction engineering, and multiphase system design. The authors highlighted the importance of continued development in this area and the need to strengthen links between fundamental research and industrial applications.

The event brought together representatives of the academia, research institutions, and industry, and underscored the importance of preserving and promoting the scientific achievements of the Serbian school of chemical engineering. The enduring value of scientific monographs as lasting sources of knowledge and as foundations for the educating future generations of researchers was also recognized.

Academician Prof. Dr. Vlada B. Veljković, one of the authors of the monograph, is the current President of the Association of Chemical Engineers of Serbia (AChE) and, since 2007, has served as the Editor-in-Chief of the journal Chemical Industry & Chemical Engineering Quarterly (CI&CEQ), which is published by AChE. Prof. Dr. Dejan U. Skala, also one of the authors, served as President of AChE from 2016 to 2025 and as Editor-in-Chief of the journals Hemijska industrija (1994-2005) and CI&CEQ (2005-2007). Prof. Dr. Ivana Banković Ilić serves as Section Editor of the journal Hemijska industrija, Editor-in-Chief of the journal Advanced Technologies (published by the Faculty of Technology in Leskovac), and President of the AChE branch in Leskovac. Their contributions of these authors have played, and continue to play, a significant role in the advancement, networking, and promotion of chemical engineering in Serbia.

The monograph “*Hydrodynamics and Mass Transfer of Multiphase Reciprocating Plate Columns”* stands as a lasting record of key achievements in the field of multiphase systems and further affirms the significant contributions of Serbian researchers to contemporary chemical engineering.